

3-Amino-7-phthalazinylbenzoisoxazoles as a Novel Class of Potent, Selective, and Orally Available Inhibitors of p38 α Mitogen-Activated Protein Kinase[†]

Liping H. Pettus,^{*,‡} Shimin Xu,[‡] Guo-Qiang Cao,[‡] Partha P. Chakrabarti,[‡] Robert M. Rzasa,[‡] Kelvin Sham,[‡] Ryan P. Wurz,[‡] Dawei Zhang,[‡] Scott Middleton,[§] Bradley Henkle,[§] Matthew H. Plant,[§] Christiaan J. M. Saris,[§] Lisa Sherman,[§] Lu Min Wong,[§] David A. Powers,[#] Yanyan Tudor,[#] Violeta Yu,[#] Matthew R. Lee,[‡] Rashid Syed,[‡] Faye Hsieh,[‡] and Andrew S. Tasker[‡]

Departments of Chemistry Research and Discovery, Inflammation, HTS Molecular Pharmacology, Molecular Structure, and Pharmacokinetics and Drug Metabolism, Amgen Inc., One Amgen Center Drive, Thousand Oaks, California 91320

Received May 9, 2008

The p38 mitogen-activated protein kinase (MAPK) is a central signaling molecule in many proinflammatory pathways, regulating the cellular response to a multitude of external stimuli including heat, ultraviolet radiation, osmotic shock, and a variety of cytokines especially interleukin-1 β and tumor necrosis factor α . Thus, inhibitors of this enzyme are postulated to have significant therapeutic potential for the treatment of rheumatoid arthritis, inflammatory bowel disease, osteoporosis, and many other diseases where aberrant cytokine signaling is the driver of disease. Herein, we describe a novel class of 3-amino-7-phthalazinylbenzoisoxazole-based inhibitors. With relatively low molecular weight, these compounds are highly potent in enzyme and cell-based assays, with minimal protein shift in 50% human whole blood. Compound **3c** was efficacious (ED₅₀ = 0.05 mg/kg) in the rat collagen induced arthritis (CIA) model.

Introduction

p38 α mitogen-activated protein kinase (MAPK^a) has been shown to play a crucial role in regulating the biosynthesis of proinflammatory cytokines including tumor necrosis factor α (TNF α) and interleukin-1 β (IL-1 β).¹ Excessive production of these two cytokines is implicated in many inflammatory diseases,² and their inhibition is a proven therapeutic strategy in suppressing inflammation. Etanercept (a soluble TNF α receptor), infliximab (a TNF α antibody), and adalimumab (a TNF α antibody) are proven to be clinically effective in the treatment of rheumatoid arthritis (RA), ankylosing spondylitis, Crohn's disease, and psoriasis by the blockade of TNF α function.³ Therefore, the discovery and development of orally active p38 MAP kinase inhibitors for the treatment of numerous inflammatory diseases have been pursued by many pharmaceutical research groups.⁴

In our preceding communication, we reported the discovery of 4-methyl-3-phthalazinylbenzamide **1** (Figure 1) as a potent and selective p38 inhibitor.⁵ The crystal structure of p38 α /compound **1** complex reveals that the binding interaction of **1** and the p38 α enzyme includes four H-bonding interactions: the cyclopropylamide carbonyl oxygen and the backbone NH of Asp168, the cyclopropylamide NH and the carboxylate of Glu71 located on the C-helix, the phthalazine ring nitrogen (N3) and the linker NH of Met109, and a second ring nitrogen (N2) intended to engage the NH of the flipped Gly110.⁶ The C₁-o-

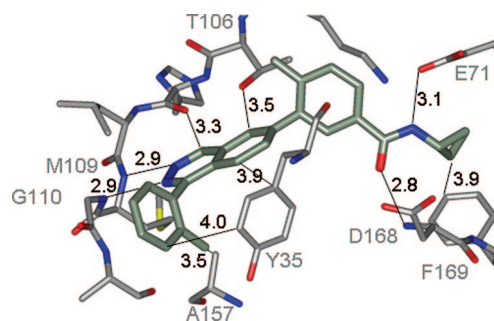


Figure 1. X-ray crystal structure of compound **1** bound in the ATP binding site of unphosphorylated p38 α . Bond distances are given in angstroms. For the inhibitor, color-coding is as follows: C, green; N, blue; O, red.

tolyl group, necessarily oriented 90° to the phthalazine ring, has a hydrophobic interaction with Ala157 (rare as a floor residue in the ATP binding site)⁷ that is drawn upward to meet the inhibitor. Moreover, flipping Gly110 induces a conformational change in the backbone of the two residues Ala111 and Asp 112, creating a narrow channel that is optimally occupied by the C₁-o-tolyl. In addition, the CH₃-group in the benzamide moiety occupies the Thr106 “gatekeeper pocket”. Finally the cyclopropyl group is nested against Phe169 that resides DFG-in.⁸ These strong interactions make for a highly potent (K_i = 0.4 nM) and selective p38 inhibitor.

To identify novel chemotypes with potentially improved physical properties and PKDM profiles, we sought to replace the benzamide moiety in compound **1** with an appropriate bioisostere while still maintaining the good potency and selectivity that compound **1** possesses (Figure 2). From the X-ray structure, we recognized that the carbonyl oxygen utilized the lone pair of electrons that were syn to the cyclopropylamine moiety to engage the NH of Asp168. Conceptually, a benzamide bioisostere that fused the carbonyl group to the benzene ring would still have a lone pair of electrons in the right trajectory for H-bonding with Asp168. Moreover, the cycle would need to be small and lipophilic to be tolerated by the preceding

[†] Atomic coordinates and structure factors for crystal structure of compound **1** with p38 α can be accessed using PDB code 3DS6.

* To whom correspondence should be addressed. Phone: 805-447-6964. Fax: 805-480-1337. E-mail: lpettus@amgen.com.

[‡] Department of Chemistry Research and Discovery.

[§] Department of Inflammation.

[#] Department of HTS Molecular Pharmacology.

[‡] Department of Molecular Structure.

[‡] Department of Pharmacokinetics and Drug Metabolism.

^a Abbreviations: AUC, area under the curve; CIA, collagen-induced arthritis; DFG, Asp-Phe-Gly sequence in ATP binding site; hWB, human whole blood; IL, interleukin; MAPK, mitogen-activated protein kinase; RA, rheumatoid arthritis; THP1, human acute monocytic leukemia cell line; TNF α , tumor necrosis factor α ; hERG, human ether-a-go-go related gene.

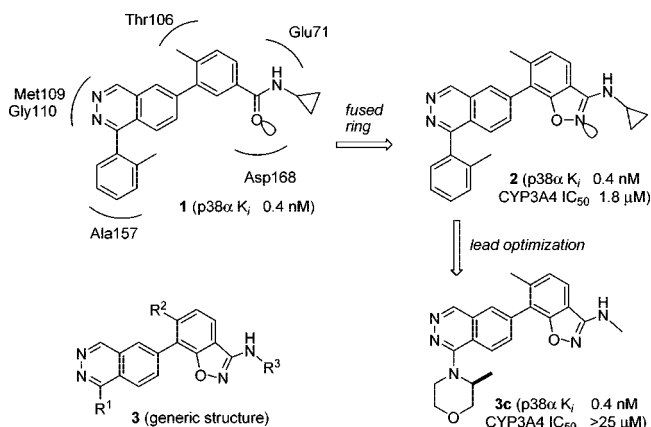


Figure 2. Benzoisoxazole as a benzamide bioisostere.

Leu167. Upon replacement of the benzamide group present in compound **1** with a benzoisoxazole, compound **2** was found to inhibit p38 α in the low nanomolar range. Herein, we report the synthesis and biological evaluation of a unique class of 3-amino-7-phthalazinylbenzoisoxazole derivatives **3** (Figure 2) as inhibitors of p38 MAP kinase.^{5b} Since several molecules in this series were burdened with moderate to strong CYP3A4 inhibition, lead optimization was focused on selecting compounds that were not only potent but also free of CYP3A4 inhibition issues. Compound **3c**, in particular, showed good efficacy (ED₅₀ = 0.05 mg/kg) in the rat collagen induced arthritis (CIA) model.

Chemistry

The synthesis of compound **2** is shown in Scheme 1. The known 1,6-dichlorophthalazine^{5b,9} (**4**) underwent selective Suzuki coupling at its C₁-Cl site with *o*-tolylboronic acid to afford the 6-chloro-1-*o*-tolylphthalazine **5**, which was then converted to the 1-*o*-tolylphthalazin-6-ylboronic acid **6** according to the Miyaura protocol.¹⁰ Boronic acid **6** participated in a Suzuki coupling reaction with the *N*-cyclopropyl-7-iodo-6-methylbenzo[*d*]isoxazol-3-amine **27** (see Scheme 3) in the presence of tetrakis(triphenylphosphine)palladium(0) to furnish compound **2**.

Other phthalazinylbenzoisoxazole analogues were prepared in a fashion similar to that described for compound **2**, differing only in the preparation of their precursors: the phthalazinylboronic acids **9–14**, boronic ester **15**, and the 7-iodobenzoisoxazoles **27–31**, **36**, and **37** (Scheme 2). Amination of the known 6-bromo-1-chlorophthalazine^{5b,9} (**7**) afforded the 6-bromo-1-aminophthalazines **8a–e**, which were then transformed into boronic acids **9–13** using Miyaura's conditions followed by acid hydrolysis. In a similar fashion, boronic acid **14** was derived from 6-bromo-1-isopropoxyphthalazine **8f**, which in turn was obtained from the etherification of compound **7** with isopropanol upon treatment with sodium hydride in THF. The iron-catalyzed cross-coupling¹¹ of the known 1-chloro-6-methoxyphthalazine (**16**)^{5b,9} with isopropylmagnesium chloride followed by demethylation using BBr₃ in dichloroethane afforded compound **18**. Triflation of this phenol and subsequent conversion of the triflate **19** to the boronic ester under Miyaura's conditions furnished 1-isopropylphthalazin-6-ylboronic ester **15**.

The synthesis of *N*-cyclopropyl-, *N*-ethyl-, and *N*-methyl-7-iodo-6-methylbenzo[*d*]isoxazol-3-amine (**27**, **28**, and **29**) is outlined in Scheme 3. Lithiation of the commercially available 2-fluoro-4-methylbenzonitrile **21** followed by iodination afforded the 2-fluoro-3-iodo-4-methylbenzonitrile **22**. Next, the nitrile group was subjected to acid hydrolysis, borane–DMS complex

reduction, and subsequent oxidation to provide the aldehyde **24**. Condensation of the aldehyde **24** with hydroxylamine afforded oxime **25**. Oxidation of **25** with *N*-chlorosuccinimide (NCS) gave the corresponding benzoyl chloride oxime, which was treated with an amine to produce compounds **26a–c**. Heating of benzoxamidines **26a–c** with 1,8-diazabicyclo[5.4.0]-undec-7-ene (DBU) in THF in a microwave provided the desired 7-iodobenzoisoxazoles **27–29**.¹²

As the need for greater quantities of 7-iodo-6-methylbenzo[*d*]isoxazol-3-amine **29** emerged, an alternative synthetic route that required no microwave heating was developed. Thus, a one-pot cyclization of ortho substituted benzonitriles to 3-amino-1,2-benzoisoxazoles, as developed by Palermo,¹³ was employed to convert benzonitrile **22** into 7-iodo-6-methylbenzo[*d*]isoxazol-3-amine **30**. Compound **30** was sequentially treated with trifluoroacetic anhydride, alkylated with dimethyl sulfate, and hydrolyzed in basic medium (NaOH) to produce 7-iodo-*N*,6-dimethylbenzo[*d*]isoxazol-3-amine **29**. The reaction of compound **30** with acetyl chloride provided amide **31**.

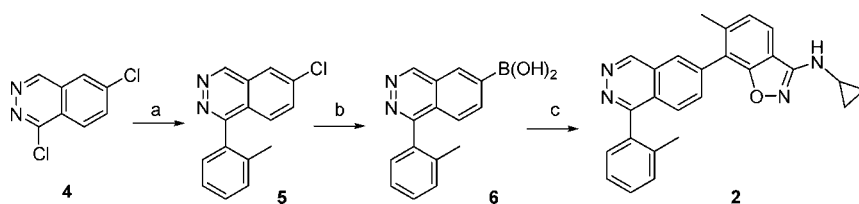
The synthesis of 3-amino-6-chloro-7-iodobenzoisoxazoles **36** and **37** is illustrated in Scheme 4. Benzyl alcohol **32** was protected with a *tert*-butyldimethylsilyl (TBDMS) group. Lithiation of compound **33** and quenching with iodine afforded compound **34**, from which the hydroxyl protecting group was removed with tetrabutylammonium fluoride (TBAF) to give benzyl alcohol **35**. Compound **35** was converted to benzoisoxazoles **36** and **37** via a five-step procedure similar to that described in Scheme 3 for compounds **27–29**.

Scheme 5 outlines the synthesis of phthalazinylindazole **40** and phthalazinylbenzoisothiazole **41**. Heating of the benzonitrile **22** with hydrazine in refluxing THF provided the 7-iodo-6-methyl-1*H*-indazol-3-amine **38**. In a similar fashion, heating of benzonitrile **22** with sulfur and ammonium hydroxide in 2-methoxyethanol gave the 3-aminobenzoisothiazole **39**.¹⁴ Treatment of compounds **38** and **39** with the (*S*)-1-(3-methylmorpholino)phthalazin-6-ylboronic acid **9** under Suzuki conditions led to compounds **40** and **41**, respectively.

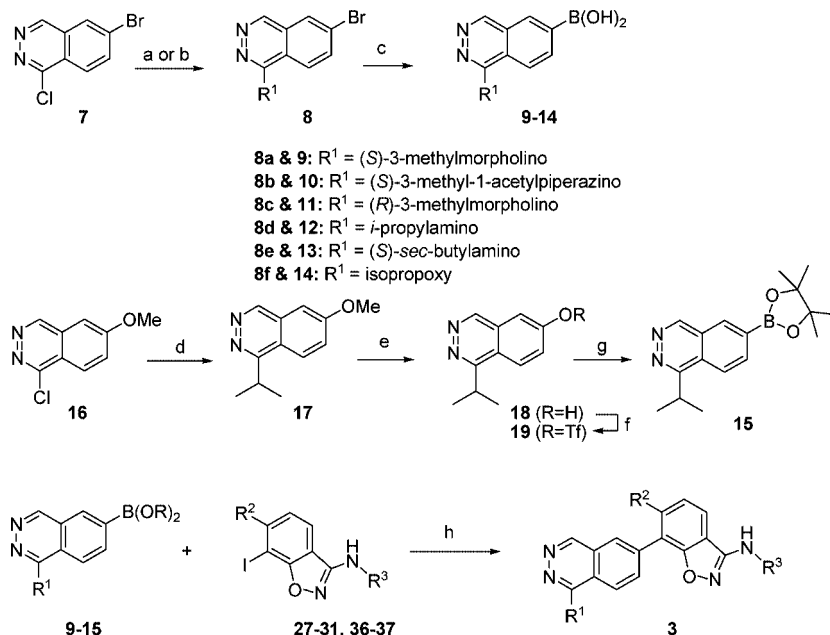
Results and Discussion

In Vitro SAR. Compounds were evaluated for their ability to inhibit the phosphorylation of substrate activating transcription factor 2 (ATF2) by recombinant human p38 α and LPS-induced TNF α production in THP1 cells. Compounds were further evaluated against TNF α -induced IL-8 production in human whole blood, an assay that was used as one of the major drivers for compound selection. This assay was a more meaningful measurement of inhibitor potency in a physiologically relevant environment because of the presence of serum albumin and other proteins.

Phthalazinylbenzoisoxazole inhibitors offered two major sites for SAR modification (R¹ and R³ in the generic structure **3**, Figure 2). To exemplify the influence induced by the R¹ group, R³ was maintained as the cyclopropyl group (Table 1). Compound **2**, (*S*)-3-methylmorpholino derivative **3a**, piperazine analogue **3f**, and isopropylamino analogue **3g** were nearly equipotent in p38 α enzyme, THP1 cell-based and whole blood TNF/IL8 assays. Although all of the compounds in Table 1 had no interference with CYP2D6 (IC₅₀ > 25 μ M), they were strong-to-moderate inhibitors of CYP3A4 (IC₅₀ = 1.8–5.6 μ M). Since CYP inhibition has a possibility of causing serious drug–drug interactions and liver toxicity in clinical use,¹⁵ the CYP3A4 inhibition was a concern for compounds made to date in this series. Compound **2**, the most hydrophobic (cLogP = 5.0) among the four compounds in Table 1, had the strongest

Scheme 1^a

^a Reagents and conditions: (a) *o*-tolylboronic acid, Pd(PPh₃)₄, 2 N Na₂CO₃, dioxane/EtOH, microwave, 78 °C, 53%; (b) (i) bis(pinacolato)diboron, Pd₂(dba)₃, KOAc, P(Cy)₃, dioxane, microwave, 120 °C; (ii) 2 N HCl, 38%; (c) compound 27, Pd(PPh₃)₄, 2 N Na₂CO₃, dioxane, microwave, 125 °C, 82%.

Scheme 2^a

- 3a** R¹ = (*S*)-3-methylmorpholino; R² = CH₃; R³ = cyclopropyl;
3b R¹ = (*S*)-3-methylmorpholino; R² = CH₃; R³ = Et;
3c R¹ = (*S*)-3-methylmorpholino; R² = CH₃; R³ = CH₃;
3d R¹ = (*S*)-3-methylmorpholino; R² = CH₃; R³ = H;
3e R¹ = (*S*)-3-methylmorpholino; R² = CH₃; R³ = acetyl;
3f R¹ = (*S*)-3-methyl-1-acetylpiperazino; R² = CH₃; R³ = cyclopropyl;
3g R¹ = isopropylamino; R² = CH₃; R³ = cyclopropyl;
3h R¹ = (*S*)-3-methylmorpholino; R² = Cl; R³ = CH₃;
3i R¹ = (*S*)-3-methylmorpholino; R² = Cl; R³ = isopropyl;
3j R¹ = (*R*)-3-methylmorpholino; R² = CH₃; R³ = CH₃;
3k R¹ = isopropylamino; R² = CH₃; R³ = CH₃;
3l R¹ = (*S*)-*sec*-butylamino; R² = CH₃; R³ = CH₃;
3m R¹ = isopropoxy; R² = CH₃; R³ = CH₃;
3n R¹ = isopropyl; R² = CH₃; R³ = CH₃;

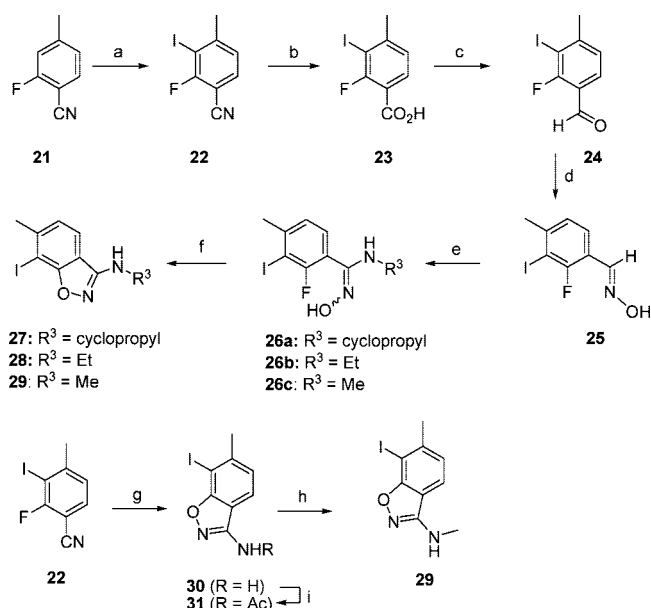
^a Reagents and conditions: (a) HNR⁴R⁵, NMP, 165 °C; (b) isopropanol, NaH, THF; (c) (i) bis(pinacolato)diboron, Pd(dppf)Cl₂, KOAc, dioxane, microwave, 120 °C; (ii) 2 N HCl; (d) Me₂CHMgCl, 0.2 equiv of Fe(acac)₃, room temp, 43%; (e) BBr₃, DCE, 74%; (f) PhN(Tf)₂, Et₃N, CHCl₃, 78%; (g) bis(pinacolato)diboron, Pd(dppf)Cl₂, KOAc, DMF, 80 °C, 40%; (h) Pd(PPh₃)₃, Na₂CO₃, dioxane, water, microwave, 120 °C.

CYP3A4 inhibition (IC₅₀ = 1.8 μM). However, a more general correlation of the CYP3A4 affinity to the lipophilicity of the inhibitor could not be made. The piperazine analogue **3f**, with the smallest cLogP of 2, still had an IC₅₀ of 4.2 μM for CYP3A4. The apparent cause of the CYP3A4 inhibition was not clear to us. We thus undertook a structure–activity study varying both termini of structure **3** (Figure 2) to identify compounds potent on the target but devoid of CYP inhibitory activity.

The effect of R² and R³ groups on the p38α inhibitory activity was studied while the R¹ group was maintained as the (*S*)-3-methylmorpholino group (Table 2). When R² was a methyl, small hydrophobic groups such as cyclopropyl, ethyl, methyl, acetyl, and hydrogen were all well tolerated at the R³ site. Compounds **3a–e** proved to be equally potent in the enzyme

assay (K_i in the range of 0.3–0.7 nM). The decrease in cell permeability on compound **3d** may be attributed to the overall increase in its polar surface area (PSA = 90.3), as compared to the ethyl analogue **3b** (PSA = 76.3). Compound **3d** also demonstrated the weakest potency in the whole blood TNFα/IL-8 assay (IC₅₀ = 5.2 nM). From this study, we also noticed that the variation of R³ group had a strong influence on the CYP3A4 inhibitory activity. While the methyl analogue **3c** and the acetyl compound **3e** did not present any potential issues with CYP3A4 inhibition (IC₅₀ > 25 μM), the ethyl analogue **3b** and the cyclopropyl analogue **3a** showed increased inhibition.

With replacement of the R² methyl group with a chloride, compounds **3h** and **3i** had comparable p38α enzyme inhibitory activity to the methyl analogues **3a** and **3c**. Unfortunately,

Scheme 3^a

^a Reagents and conditions: (a) LiTMP, I₂, 48%; (b) H₂SO₄, dioxane, 92%; (c) (i) BH₃-SMe₂, B(OMe)₃, THF, 89%; (ii) MnO₂, CH₂Cl₂, 89%; (d) NH₂OH, EtOH, 85%; (e) (i) NCS, DMF, 55 °C; (ii) R³NH₂, THF; (f) DBU, THF/NMP, 150 °C, 70 min, microwave; (g) acetohydroxamic acid, KO^tBu, DMF, 69%; (h) (i) (CF₃CO₂)₂O, CH₂Cl₂; (ii) K₂CO₃, Me₂SO₄; (iii) NaOH, MeOH, 68% for three steps; (i) Cs₂CO₃, AcCl, CH₂Cl₂, 92%.

compounds **3h** and **3i** were also burdened with the issue of moderate CYP3A4 inhibition (IC₅₀ = 4.5–6.0 μM).

The observation that compounds **3c** and **3e** were devoid of CYP3A4 inhibition (IC₅₀ > 25 μM) was encouraging. As shown in Table 3, we focused our efforts on the modification of R¹ to determine if other substituents were well tolerated when R³ was fixed as a methyl group. The (*R*)-3-methylmorpholine analogue **3j**, isopropylamino compound **3k**, and (*S*)-*sec*-butylamino derivative **3l** were equipotent to the (*S*)-3-methylmorpholine analogue **3c** in terms of p38α inhibition. The isopropyl ether **3m** and the isopropyl analogue **3n**, which were less polar than the amino analogues, showed comparable THP1 cell based potency. More significantly, however, was the observation that all compounds in Table 3, regardless of their lipophilicity (cLogP), had little CYP3A4 inhibition (IC₅₀ > 25 μM). This fact implied that the R¹ substituents had little to no influence on CYP inhibition when R³ was a methyl group. On the basis of these findings, modification of R¹ substituents appeared to be a promising approach for improving PKDM profiles while maintaining good potency on both p38α enzyme and cell based assays.

After optimization of R¹ and R³ groups, an investigation of possible replacement for the benzoisoxazole subunit was undertaken. To facilitate this study, R¹ was selected as (*S*)-3-methylmorpholine and R³ was fixed as a hydrogen atom (for synthetic simplicity). The benzoisoxazole ring oxygen was replaced with either a sulfur atom or a NH group (Table 4). Compared to the benzoisoxazole **3d**, the indazole **40** and the benzoisothiazole **41** showed a 50-fold and 7-fold potency loss in p38α enzyme inhibition, respectively. These observations supported our original hypothesis in that the cycle would need to be small and lipophilic to be tolerated by the Leu167 residue in the protein. Molecular modeling (FLAME)¹⁶ of compound **3c** in the ATP binding site of unphosphorylated p38α (Figure 3) shows that the O-atom in the benzoisoxazole ring is in close contact with the Leu167 residue in the protein. For the indazole

40, the polar NH appears to be less tolerated by the aforementioned leucine, and for compound **41**, the increased ring size of the benzoisothiazole appears to create unfavorable steric interaction with the leucine residue.

Pharmacokinetic (PK) studies carried out in Sprague–Dawley rats on compounds **3c** and **3j–n** ultimately resulted in the selection of **3c** for further profiling. **3c** displayed superior PK properties evidenced by lower clearance and higher bioavailability than analogs **3j–n**. By intravenous (iv) administration of 2 mg/kg, **3c** showed a clearance of 1447 (mL/h)/kg, a moderate volume of distribution of 2401 mL/kg, and an elimination half-life of 2.8 h. Compound **3c** was well-absorbed (*t*_{max} = 1.7 h, *C*_{max} = 1040 ng/mL) following oral administration of 10 mg/kg [a solution dose in 1% Tween-80 in OralPlus (pH 2.2)], with an oral bioavailability (*F*) of 67%. Compound **3c** was 90% and 92% bound to rat and human plasma protein, respectively (determined by the ultrafiltration methods). In rat and human liver microsomes, **3c** had a metabolic rate of 120 and 132 (μL/min)/(mg of protein), respectively.¹⁷

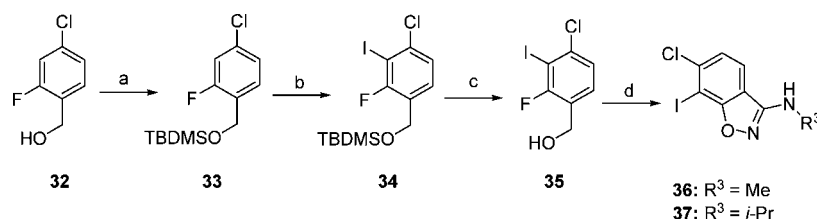
To evaluate kinase selectivity, compound **3c** was tested for inhibitory activity versus 32 kinases.¹⁸ With the exception of p38β (*K*_i = 1.8 nM), compound **3c** (p38α, *K*_i = 0.4 nM) showed > 1000-fold selectivity against all other kinases evaluated. As commonly reported for p38α inhibitors,¹⁹ **3c** was selective against p38γ and p38δ isoforms but not against p38β. In a broader selectivity screen against a variety of G-protein-coupled receptors and ion channels, **3c** did not exhibit any off-target interactions when tested at 10 μM concentration. Additional profiling of **3c** showed that it neither induced LDH release nor caused human pregnane X receptor (hPXR) trans-activation. In addition, it yielded an IC₅₀ of 13 μM for blockade of the hERG cardiac channel determined by manual electrophysiology. In view of its promising pharmacokinetic and selectivity profiles, **3c** was further evaluated in an animal disease model.

While an X-ray structure shows that benzamide **1** binds to the ATP binding site in p38α protein (Figure 1), these data do not exist for the benzoisoxazoles. Therefore, we undertook classical Michaelis–Menten kinetic characterization of the benzoisoxazoles,²⁰ using **3c** as a representative example. The kinetic data of **3c**, shown in Figures 4 and 5 and Table 5, confirmed that **3c** was an ATP competitive inhibitor of p38α kinase. As for a competitive inhibitor, the *V*_{max} does not vary significantly while the ATP apparent *K*_m shows the expected linear relationship with concentration of **3c**.

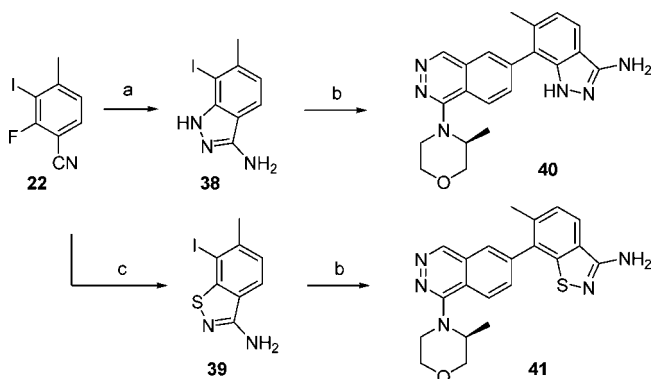
In Vivo Pharmacology. The rat collagen induced arthritis (CIA) model was chosen as the animal rheumatoid arthritis disease model.²¹ Compound **3c** was administered at 0.03, 0.1, 0.3, 1.0, and 3.0 mg/kg once a day to rats, beginning on day 10 through day 17 following immunization. As shown in Figure 6, **3c** inhibited paw swelling in the CIA model in a dose dependent manner with an ED₅₀ of 0.05 mg/kg, corresponding to an exposure of AUC (0–24 h) = 22.4 nM·h, with an interpolated *C*_{max} and *C*_{24h} of 7.0 and 0.3 nM, respectively.

Conclusion

A structurally novel phthalazinylbenzoisoxazole series has been discovered as p38 MAP kinase inhibitors. Structural biology guided the design and modification for this series of compounds. Through SAR studies, analogues with high affinity to the p38 MAP kinase and no considerable CYP3A4 inhibition were identified. As a representative example, optimized analogue **3c** was potent and selective in vitro. Furthermore, with a

Scheme 4^a

^a Reagents and conditions: (a) TBDMSCl, imidazole, CH₂Cl₂, 84%; (b) LDA, I₂, THF, 84%; (c) TBAF, THF, 97%; (d) (i) MnO₂, CH₂Cl₂; (ii) NH₂OH, EtOH; (iii) NCS, DMF; (iv) R³NH₂, THF; (v) DBU, THF/NMP, microwave, 165 °C.

Scheme 5^a

^a Reagents and conditions: (a) hydrazine hydrate, THF, reflux, 90%; (b) compound **9**, Pd(PPh₃)₄, Na₂CO₃, dioxane, water, microwave, 120 °C; (c) S₈, NH₄OH, MeOCH₂CH₂OH, 130 °C, 31%.

Table 1. SAR: Variation of the R¹ Substituent^a

compd	R ¹	p38α K _i (nM)	THP1 LPS/TNFα IC ₅₀ (nM)	hWB TNFα/IL-8 IC ₅₀ (nM)	CYP 3A4 IC ₅₀ (μM)	cLogP ^b
2		0.4	0.4	3.3	1.8	5.0
3a		0.7	0.6	1.8	5.6	3.9
3f		0.8	0.8	1.4	4.2	2.0
3g		0.5	0.4	0.7	5.6	4.4

^a The p38α K_i and IC₅₀ of cell based assays are mean values derived from at least three independent dose–response curves. Variability around the mean value was <50%. Midazolam was the substrate in CYP3A4 inhibition assay. ^b Physicochemical properties were calculated using the Daylight Toolkit,²² within Amgen's proprietary software (ADAAPT).²³

desirable pharmacokinetic profile, compound **3c** exhibited efficacy (ED₅₀ of 0.05 mg/kg) in a rat collagen induced arthritis model.

Experimental Section

Chemistry. All reagents and solvents were obtained from commercial suppliers and used without further purification. All reactions were carried out under an inert atmosphere of nitrogen unless otherwise noted. All microwave-assisted reactions were

Table 2. SAR: Influence of the R² and R³ Substituents^a

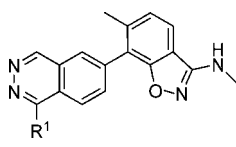
compd	R ²	R ³	THP1		hWB	CYP3A4
			p38α K _i (nM)	LPS/TNFα IC ₅₀ (nM)	TNFα/IL-8 IC ₅₀ (nM)	IC ₅₀ (μM)
3a	Me	cyclopropyl	0.7	0.6	1.3	5.6
3b	Me	Et	0.3	0.4	2.0	10
3c	Me	Me	0.4	0.4	3.3	>25
3d	Me	H	0.3	3.6	5.2	12
3e	Me	acetyl	0.6	0.7	2.0	>25
3h	Cl	Me	0.2	1.3	3.3	6.0
3i	Cl	<i>i</i> -Pr	0.4	3.6	15	4.5

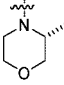
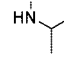
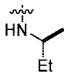
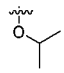
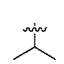
^a The p38α K_i and IC₅₀ of cell based assays are mean values derived from at least three independent dose–response curves. Variability around the mean value was <50%. Midazolam was the substrate in CYP3A4 inhibition assay.

conducted with a Smith synthesizer from Personal Chemistry, Uppsala, Sweden. Silica gel chromatography was performed using either glass columns packed with silica gel (200–400 mesh, Aldrich Chemical) or prepacked silica gel cartridges (Biotage and ISCO). ¹H NMR spectra were obtained on a Bruker DRX 400 (400 MHz) spectrometer and reported as ppm downfield from tetramethylsilane. All final compounds were purified to >95% purity as determined by LCMS analysis obtained on Agilent 1100; conditions are listed in the Supporting Information. Low-resolution mass spectral (MS) data were determined on a Perkin-Elmer SCIEX API 165 mass spectrometer using ES ionization modes (positive or negative). High-resolution mass spectral (MS) data were obtained on a Agilent Technologies Mass Hunter ES-TOF Tuning Mix mass spectrometer.

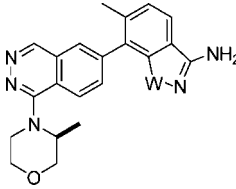
1-*o*-Tolylphthalazin-6-ylboronic Acid (6). To a mixture of 1,6-dichlorophthalazine (**4**) (1.03 g, 5.21 mmol), *o*-tolylboronic acid (0.57 g, 4.17 mmol) and tetrakis(triphenylphosphine)palladium(0) (301 mg, 0.26 mmol) in 1,4-dioxane (7.5 mL) in a 20 mL glass tube was added 2.5 mL of EtOH, followed by 5 mL of 2 N Na₂CO₃. The glass tube was sealed and heated in a Personal Chemistry microwave at 78 °C for 45 min. The mixture was treated with 10 mL of 1 N NaOH and extracted with EtOAc (2 × 35 mL). The combined EtOAc layers were dried and concentrated. Purification on silica gel chromatography (eluted with 30–75% EtOAc in hexanes) provided 6-chloro-1-*o*-tolylphthalazine (**5**) (543 mg, 53% yield) as a brown amorphous solid. ¹H NMR (DMSO-*d*₆): δ 2.0 (s, 3H), 7.15–7.55 (m, 5H), 7.99 (d, *J* = 9.0 Hz, 1H), 8.44 (s, 1H), 9.73 (s, 1H). MS (ESI, positive ion) *m/z*: 255 (M + 1).

In a sealed glass tube, a mixture of 6-chloro-1-*o*-tolylphthalazine (127 mg, 0.50 mmol), bis(pinacolato)diboron (146 mg, 0.57 mmol), potassium acetate (98 mg, 1.00 mmol), tris(dibenzylideneacetone)dipalladium(0) (18 mg, 0.02 mmol), and tricyclohexylphosphine (11 mg, 0.04 mmol) in 2 mL of 1,4-dioxane was heated in a Personal Chemistry microwave at 120 °C for 30 min. The reaction mixture was diluted with 1 mL of dioxane, filtered through a pad

Table 3. Variation of R¹-Phthalazinyl-N,6-dimethylbenzo[d]isoxazol-3-amine^a


compd	R ¹	THP1		hWB		CYP3A4	cLogP
		p38α K _i (nM)	LPS/TNFα IC ₅₀ (nM)	TNFα/IL-8 IC ₅₀ (nM)	CYP3A4 IC ₅₀ (μM)		
3j		0.3	1.0	4.5	>25	3.5	
3k		0.5	0.7	2.2	>25	4.1	
3l		0.2	1.3	2.1	>25	4.7	
3m		0.4	0.7	7.0	>25	3.9	
3n		1.1	1.1	3.4	>25	3.7	

^a The p38α K_i and IC₅₀ of cell based assays are mean values derived from at least three independent dose–response curves. Variability around the mean value was <50%. Midazolam was the substrate in CYP3A4 inhibition assay.

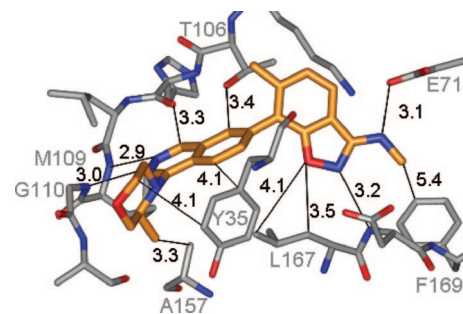
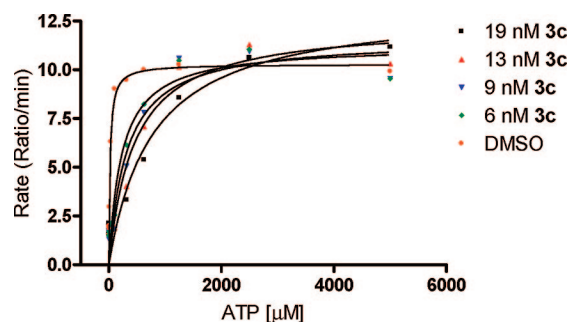
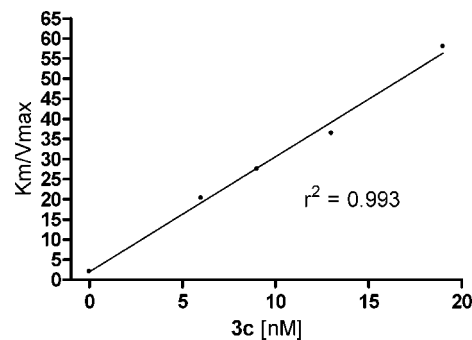
Table 4. SAR: Replacement of the Benzoisoxazole Ring^a


compd	W	p38α	THP1	LPS/TNFα	hWB	TNFα/IL8	CYP 3A4
		K _i (nM)	IC ₅₀ (nM)	IC ₅₀ (nM)	IC ₅₀ (nM)	IC ₅₀ (μM)	
3d	O	0.3	3.6	5.2	12		
40	NH	16	120	153	NT ^b		
41	S	2.0	29	50	4.0		

^a The p38α K_i and IC₅₀ of cell based assays are mean values derived from at least three independent dose–response curves. Variability around the mean value was <50%. Midazolam was the substrate in CYP3A4 inhibition assay. ^b NT: not tested.

of Celite, and rinsed with 5 mL of EtOAc. The filtrate was concentrated, and the dark residue was treated with 2 mL of 2 N HCl. Hexanes (5 mL) were added, and the mixture was sonicated for 5 min. The hexanes layer was discarded. The remaining acidic layer was diluted with 1 mL of DMSO and loaded on a reverse phase HPLC [using a gradient of 10–60% of (0.1% of trifluoroacetic acid in acetonitrile) in (0.1% of trifluoroacetic acid in water)]. The 1-*o*-tolylphthalazin-6-ylboronic acid (**6**) (50 mg, 38% yield) was obtained as a white fluffy solid after drying the HPLC fractions in a lyophilizer. ¹H NMR (DMSO-*d*₆): δ 2.01 (s, 3H), 7.19–7.55 (m, 5H), 8.30 (d, *J* = 8.2 Hz, 1H), 8.65 (s, 1H), 9.76 (s, 1H). MS (ESI, positive ion) *m/z*: 265 (M + 1).

N-Cyclopropyl-6-methyl-7-(1-*o*-tolylphthalazin-6-yl)benzo[d]isoxazol-3-amine (2). In a sealed glass tube, a mixture of *N*-cyclopropyl-7-iodo-6-methylbenzo[d]isoxazol-3-amine (**27**) (52 mg, 0.16 mmol), 1-*o*-tolylphthalazin-6-ylboronic acid (**6**) (32 mg, 0.18 mmol), tetrakis(triphenylphosphine)palladium(0) (7.7 mg, 0.006 mmol) in 0.8 mL of 1,4-dioxane and aqueous solution of

**Figure 3.** Molecular modeling of compound **3c** in the ATP binding site of unphosphorylated p38α. Note that the O-atom of the benzoisoxazole ring is in close contact with L167. Bond distances are given in angstroms. For the inhibitor, color coding is as follows: C, gold; N, blue; O, red.**Figure 4.** Michaelis–Menten plot for **3c**.**Figure 5.** K_m/V_{max} vs concentration of **3c** (nM).**Table 5.** Concentration of **3c**, V_{max}, and Apparent K_m

concn of 3c (nM)	V _{max} (ratio/min)	K _m (μM)
19	13.28	769.9
13	12.41	451.9
9	11.60	319.4
6	11.26	229.2
0	10.29	21.58

Na₂CO₃ (2 N, 0.20 mL) was heated in a Personal Chemistry microwave at 125 °C for 20 min. The mixture was treated with 1 mL of 1 N NaOH and extracted with EtOAc (3 × 5 mL). The combined EtOAc layers were dried, concentrated, and purified on a silica gel column (eluted with 2.5–15% MeOH in DCM) to provide the title compound (55 mg, 82% yield) as a light-yellow amorphous solid. ¹H NMR (CDCl₃): δ 0.87 (m, 2H), 0.72 (m, 2H), 2.19 (s, 3H), 2.42 (s, 3H), 2.88 (m, 1H), 4.75 (br s, 1H), 7.23 (m, 1H), 7.31–7.46 (m, 4H), 7.53 (d, *J* = 8.0 Hz, 1H), 7.74 (d, *J* = 8.6 Hz, 1H), 7.88 (m, 1H), 8.13 (s, 1H), 9.59 (s, 1H). MS (ESI, positive ion) *m/z*: 407 (M + 1). Anal. (C₂₆H₂₂N₄O) C, H, N.

(S)-6-Bromo-1-(3-methylmorpholino)phthalazine (8a). In a glass tube, to a solution of 6-bromo-1-chlorophthalazine (2.0 g, 8.2 mmol) and (*S*)-3-methylmorpholine (2.1 mL, 21 mmol) in 3

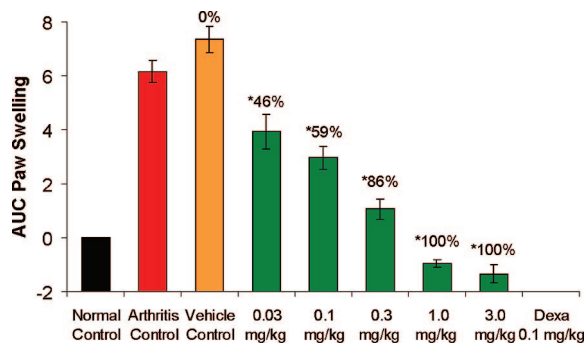


Figure 6. Effect of **3c** on CIA in Lewis rats. Arthritis was induced by intradermal injection of porcine type II collagen emulsified 1:1 in incomplete Freund's adjuvant (IFA). Animals were assigned to treatment groups at disease onset (study day 0), which occurred 10–12 days following immunization. Compound **3c** or vehicle (1% Tween-80 in Oraplus, pH 2.2) was administered orally once a day for 7 days. Dexamethasone was administered once daily, sc, for 7 days. Paw diameter was measured daily from day 0 through day 7. Area under the paw swelling curve (AUC) was calculated and used to determine percent inhibition of inflammation compared with vehicle controls. Data points represent mean \pm STE ($n = 8$ rats/group): (*) $p \leq 0.05$ vs vehicle control.

mL of NMP was added triethylamine (1.4 mL, 9.9 mmol). The glass tube was sealed, and the mixture was heated at 165 °C in an oil bath for 1 h. After cooling to room temperature, the reaction mixture was loaded onto a silica gel column. Elution with a gradient of 1–5% of (2 M NH_3 in MeOH) in DCM gave the title compound (2.07 g, 82% yield) as a yellow solid. $^1\text{H NMR}$ (CDCl_3): δ 1.19 (d, $J = 6.2$ Hz, 3H), 3.39 (m, 1H), 3.65 (m, 2H), 4.02 (m, 4H), 7.90–7.98 (m, 2H), 8.06 (d, $J = 1.8$ Hz, 1H), 9.14 (s, 1H). MS (ESI, positive ion) m/z : 310 ($M + 1$).

A similar procedure was used to prepare compounds **8b–e**.

(S)-1-(4-(6-Bromophthalazin-1-yl)-3-methylpiperazin-1-yl)-ethanone (8b). $^1\text{H NMR}$ (CDCl_3): δ 1.20 (m, 3H), 2.16 (s, 1.5H), 2.20 (s, 1.5H), 3.40–3.80 (m, 5H), 4.01–4.44 (m, 2H), 7.93 (m, 2H), 8.07 (s, 1H), 9.14 (s, 1H). MS (ESI, positive ion) m/z : 350 ($M + 1$).

(R)-6-Bromo-1-(3-methylmorpholino)phthalazine (8c). $^1\text{H NMR}$ (CDCl_3): δ 1.19 (d, $J = 6.2$ Hz, 3H), 3.39 (m, 1H), 3.65 (m, 2H), 4.02 (m, 4H), 7.90–7.98 (m, 2H), 8.06 (d, $J = 1.8$ Hz, 1H), 9.14 (s, 1H). MS (ESI, positive ion) m/z : 310 ($M + 1$).

6-Bromo-*N*-isopropylphthalazin-1-amine (8d). $^1\text{H NMR}$ (CDCl_3): δ 1.38 (d, $J = 6.5$ Hz, 6H), 4.61 (m, 1H), 4.87 (br, 1H), 7.63 (d, $J = 8.8$ Hz, 1H), 7.85 (d, $J = 8.6$ Hz, 1H), 7.95 (d, $J = 1.5$ Hz, 1H), 8.84 (s, 1H). MS (ESI, positive ion) m/z : 267 ($M + 1$).

(S)-6-Bromo-*N*-sec-butylphthalazin-1-amine (8e). $^1\text{H NMR}$ (methanol- d_4): δ 1.01 (t, $J = 7.28$ Hz, 3H), 1.32 (d, $J = 6.53$ Hz, 3H), 1.68 (sept, $J = 7.03$ Hz, 1H), 1.78 (sept, $J = 7.03$ Hz, 1H), 4.36 (sex., $J = 6.53$ Hz, 1H), 7.99 (d, $J = 8.53$ Hz, 1H), 8.14 (s, 1H), 8.21 (d, $J = 8.53$ Hz, 1H), 8.76 (s, 1H). MS (ESI, positive ion) m/z : 281 ($M + 1$).

6-Bromo-1-isopropoxyphthalazine (8f). To a solution of propan-2-ol (1.23 g, 20.53 mmol) in THF (5.0 mL) and DMF (1.5 mL) at 0 °C was added slowly sodium hydride (411 mg of 60% wt, 10.26 mmol) under a nitrogen atmosphere. The mixture was stirred at 0 °C for 10 min, and 6-bromo-1-chlorophthalazine (1.00 g, 4.10 mmol) was added as solid. After the reaction mixture was stirred at room temperature for 4 h, it was cooled with an ice bath, treated with saturated ammonium chloride (10 mL), and extracted with EtOAc (2 \times 50 mL). The combined organic phases were washed with brine (10 mL), dried over Na_2SO_4 , filtered, and concentrated. The brown residue was purified by silica gel chromatography (eluted with 30–70% EtOAc in hexanes) to give 967 mg of the title compound (88%) as an off-white amorphous solid. $^1\text{H NMR}$ (CDCl_3): δ 1.50 (d, $J = 6.0$ Hz, 6H), 5.76 (m,

1H), 7.91 (d, $J = 8.6$ Hz, 1H), 8.02 (s, 1H), 8.09 (d, $J = 8.9$ Hz, 1H), 9.07 (s, 1H). MS (ESI, positive ion) m/z : 268.0 ($M + 1$).

(S)-1-(3-Methylmorpholino)phthalazin-6-ylboronic Acid (9). A mixture of (*S*)-6-bromo-1-(3-methylmorpholino)phthalazine **8a** (1.60 g, 5.2 mmol), bis(pinacolato)diboron (2.0 g, 7.8 mmol), and potassium acetate (2.5 g, 26 mmol) in DMF (25 mL) was degassed for 20 min. It was then treated with 1,1'-bis(diphenylphosphino)ferrocenepalladium dichloride (0.38 g, 0.52 mmol). The reaction mixture was stirred at 85 °C for 18 h. After cooling to room temperature, the reaction mixture was diluted with 50 mL of EtOAc and filtered through a Celite pad. The organic solvent of the filtrate was removed in vacuo. The remaining residue was treated with 50 mL of Et_2O and 50 mL of 1 N aqueous HCl, stirred for 5 min, and filtered through a Celite pad again. The filtrate was transferred to a separatory funnel. The aqueous phase was separated, and the organic phase was washed with 10 mL of 1 N aqueous HCl. The combined aqueous phases were concentrated in vacuo. The residue was dissolved in 2.5 mL of MeOH and 2.5 mL of DMSO, purified via a reverse phase HPLC [using a gradient of 10–60% of (0.1% of trifluoroacetic acid in acetonitrile) in (0.1% of trifluoroacetic acid in water)]. The title compound (910 mg, 64% yield) was obtained as a white fluffy solid after drying the HPLC fractions in a lyophilizer. $^1\text{H NMR}$ ($\text{DMSO}-d_6$): δ 1.25 (m, 3H), 3.60–3.80 (m, 4H), 3.98 (m, 2H), 4.21 (m, 1H), 8.22 (d, $J = 9.4$ Hz, 1H), 8.41 (d, $J = 8.6$ Hz, 1H), 8.61 (s, 1H), 8.68 (br, 2H), 9.50 (s, 1H). MS (ESI, positive ion) m/z : 274 ($M + 1$).

A similar procedure was used to prepare boronic acids **10–14**.

(S)-1-(4-Acetyl-2-methylpiperazin-1-yl)phthalazin-6-ylboronic Acid (10). MS (ESI, positive ion) m/z : 315 ($M + 1$).

(R)-1-(3-Methylmorpholino)phthalazin-6-ylboronic Acid (11). $^1\text{H NMR}$ ($\text{DMSO}-d_6$): δ 1.25 (m, 3H), 3.60–3.80 (m, 4H), 3.98 (m, 2H), 4.21 (m, 1H), 8.22 (d, $J = 9.4$ Hz, 1H), 8.41 (d, $J = 8.6$ Hz, 1H), 8.61 (s, 1H), 8.68 (br, 2H), 9.50 (s, 1H). MS (ESI, positive ion) m/z : 274 ($M + 1$).

1-(Isopropylamino)phthalazin-6-ylboronic Acid (12). $^1\text{H NMR}$ ($\text{DMSO}-d_6$): δ 1.36 (t, $J = 6.2$ Hz, 6H), 4.31 (m, 1H), 8.42 (d, $J = 8.2$ Hz, 1H), 8.51 (s, 1H), 8.67 (d, $J = 8.4$ Hz, 1H), 8.75 (br, 2H), 9.01 (s, 1H), 9.21 (br, 1H). MS (ESI, positive ion) m/z : 232 ($M + 1$).

(S)-1-(sec-Butylamino)phthalazin-6-ylboronic Acid (13). $^1\text{H NMR}$ ($\text{DMSO}-d_6$): δ 0.94 (t, $J = 7.2$ Hz, 3H), 1.32 (d, $J = 6.4$ Hz, 3H), 1.64 (m, 1H), 1.76 (m, 1H), 4.21 (m, 1H), 8.41 (m, 1H), 8.48 (s, 1H), 8.68 (m, 3H), 8.98 (s, 1H), 9.18 (br, 1H). MS (ESI, positive ion) m/z : 246 ($M + 1$).

1-Isopropoxyphthalazin-6-ylboronic Acid (14). $^1\text{H NMR}$ ($\text{DMSO}-d_6$): δ 1.47 (d, $J = 6.2$ Hz, 6H), 5.60 (m, 1H), 8.16 (d, $J = 8.3$ Hz, 1H), 8.40 (d, $J = 8.0$ Hz, 1H), 8.56 (s, 1H), 8.60 (br, 2H), 9.48 (s, 1H). MS (ESI, positive ion) m/z : 233 ($M + 1$).

1-Isopropyl-6-methoxyphthalazine (17). To a solution of 1-chloro-6-methoxyphthalazine (638 mg, 3.28 mmol) and iron(III) acetylacetonate (58 mg) in tetrahydrofuran (32 mL) and 1-methyl-2-pyrrolidinone (3.2 mL) was added isopropylmagnesium chloride (2.46 mL of 2.0 M in ether, 5.92 mmol) via a syringe. The resulting mixture was stirred for 10 min, then diluted with EtOAc and carefully quenched with a few drops of 10% HCl. The mixture was washed with saturated aqueous NaHCO_3 solution. The organic layer was dried over MgSO_4 and concentrated in vacuo. Purification on an ISCO 40 g column (20–70% EtOAc in hexanes) afforded 1-isopropyl-6-methoxyphthalazine (288 mg, 43% yield) as a golden brown oil. $^1\text{H NMR}$ (CDCl_3): δ 1.53 (d, $J = 6.85$ Hz, 6H), 3.77–3.91 (m, 1H), 3.99 (s, 3H), 7.17 (d, $J = 2.35$ Hz, 1H), 7.48 (dd, $J = 9.10, 2.64$ Hz, 1H), 8.08 (d, $J = 9.19$ Hz, 1H), 9.33 (s, 1H). MS (ESI, positive ion) m/z : 203.2 ($M + 1$).

1-Isopropylphthalazin-6-ol (18). A solution of 1-isopropyl-6-methoxyphthalazine (205 mg, 1.01 mmol) in 1,2-dichloroethane (5.0 mL) was treated with boron tribromide (5.07 mL of 1.0 M solution in dichloroethane, 5.07 mmol), and the resulting golden brown mixture was stirred at 80 °C for 18 h. The cooled mixture was diluted with DCM, and the reaction was quenched with saturated aqueous NH_4Cl solution. The layers were separated, and the aqueous layer was basified to pH \sim 7 with 5 N NaOH, resulting

in the precipitation of a tan solid. Filtration, followed by drying under high vacuum overnight, afforded 1-isopropylphthalazin-6-ol (142 mg, 74% yield) as a tan solid. $^1\text{H NMR}$ (DMSO- d_6): δ 1.38 (d, $J = 6.85$ Hz, 6H), 3.73–3.99 (m, 1H), 7.26 (d, $J = 2.15$ Hz, 1H), 7.47 (dd, $J = 9.00, 2.35$ Hz, 1H), 8.19 (d, $J = 8.80$ Hz, 1H), 9.33 (s, 1H), 10.81 (br, 1H). MS (ESI, positive ion) m/z : 189.2 (M + 1).

1-Isopropylphthalazin-6-yl Trifluoromethanesulfonate (19). A mixture of 1-isopropylphthalazin-6-ol (208 mg, 1.11 mmol), *N*-phenyltrifluoromethanesulfonamide (475 mg, 1.33 mmol), *N,N*-dimethylpyridin-4-amine (13 mg), and triethylamine (0.23 mL, 1.66 mmol) was combined with chloroform (6.0 mL), and the mixture was heated at 60 °C for 2 h, during which LCMS indicated the reaction was complete. The cooled reaction mixture was diluted with CH_2Cl_2 and washed with saturated aqueous NaHCO_3 solution. The organic layer was dried over MgSO_4 , filtered, and concentrated in vacuo. Purification on an ISCO 12 g column (20–50% EtOAc in hexanes) afforded 1-isopropylphthalazin-6-yl trifluoromethanesulfonate (277 mg, 78% yield) as a maize color solid. $^1\text{H NMR}$ (CDCl_3): δ 1.56 (d, $J = 6.85$ Hz, 6H), 3.84–3.96 (m, 1H), 7.79 (dd, $J = 9.10, 2.45$ Hz, 1H), 7.87 (d, $J = 2.35$ Hz, 1H), 8.32 (d, $J = 9.19$ Hz, 1H), 9.47 (s, 1H). MS (ESI, positive ion) m/z : 321.1 (M + 1).

1-Isopropyl-6-(4,4,5,5-tetramethyl-1,3,2-dioxaborolan-2-yl)phthalazine (15). Into a 50 mL round-bottomed flask under argon were added 1-isopropylphthalazin-6-yl trifluoromethanesulfonate (269 mg, 0.84 mmol), 4,4,5,5-tetramethyl-2-(4,4,5,5-tetramethyl-1,3,2-dioxaborolan-2-yl)-1,3,2-dioxaborolane (320 mg, 1.26 mmol), dichloro[1,1'-bis(diphenylphosphino)ferrocene]palladium(II) dichloromethane adduct (61 mg, 84 μmol), and potassium acetate (412 mg, 4.2 mmol), followed by 1,4-dioxane (3.0 mL). The mixture was heated at 80 °C for 2 h. The cooled reaction mixture was diluted with EtOAc and filtered via a pad of Celite. The filtrate was extracted with 10% HCl, and the organic layer was discarded. The aqueous layer was neutralized with 1 N NaOH to pH ~ 7 , resulting in the precipitation of the title compound (99 mg, 40% yield) as a tan solid. $^1\text{H NMR}$ (methanol- d_4): δ 1.19 (s, 6H), 1.40 (s, 6H), 1.50 (d, $J = 6.6$ Hz, 6H), 4.03 (m, 1H), 8.33 (m, 3H), 9.47 (s, 1H). MS (ESI, positive ion) m/z : 299.3 (M + 1).

2-Fluoro-3-iodo-4-methylbenzonitrile (22). A solution of 2,2,6,6-tetramethyl-4-piperidine (TMP) (45 mL, 267 mmol) in THF (400 mL) was cooled below -80 °C. *n*-Butyllithium (2.5 M in hexane, 110 mL, 275 mmol) was added, slowly maintaining the temperature of the mixture below -70 °C. After the addition was completed, the reaction mixture was warmed to -50 °C and stirred at this temperature for 30 min. The clear solution became turbid, indicating salt formation. It was cooled to -80 °C again, and a solution of 2-fluoro-4-methylbenzonitrile (**21**) (32.4 g, 240 mmol) in THF (150 mL) was slowly added taking care that the temperature of the reaction mixture remained below -70 °C. It was then warmed to -50 °C and stirred for 30 min. The mixture was then cooled to -70 °C, and a saturated solution of I_2 (67 g, 264 mmol) in THF was added slowly maintaining the temperature at -70 °C. After complete addition, the mixture was warmed to ambient temperature. It was added to a solution of $\text{Na}_2\text{S}_2\text{O}_3$ (160 g in 1.5 L of water) and stirred for an hour. The organic layer was separated, and the aqueous layer was extracted with EtOAc. The organic layers were combined, washed with brine, dried over Na_2SO_4 , and filtered. The volatiles were evaporated under reduced pressure. The crude product was subjected to vacuum distillation. At about 60 °C, excess TMP was removed. At about 100 °C, the starting compound 2-fluoro-4-methylbenzonitrile and a small amount of 2-fluoro-3-iodo-4-methylbenzonitrile were removed. Finally, at 115 °C, pure 2-fluoro-3-iodo-4-methylbenzonitrile (**22**) was obtained (30 g, 48% yield) as an off-white amorphous solid upon cooling to room temperature. $^1\text{H NMR}$ (CDCl_3): δ 2.56 (s, 3H), 7.15 (d, $J = 8.0$ Hz, 1H), 7.49 (m, 1H). MS (ESI, positive ion) m/z : 261.9 (M + 1).

2-Fluoro-3-iodo-4-methylbenzoic Acid (23). A mixture of 2-fluoro-3-iodo-4-methylbenzonitrile (5.0 g, 19 mmol) in dioxane (10 mL) and 60% H_2SO_4 (10 mL) was heated at 115 °C in an oil bath for 18 h. After the mixture was cooled to room temperature,

it was poured onto 30 g of ice. The tan solid was filtered, washed with water (2×5 mL) followed by EtOAc (2×30 mL), then collected and dried to afford 2-fluoro-3-iodo-4-methylbenzoic acid (3.3 g, LCMS >95% pure) as a tan crystalline solid. The filtrate was transferred to a separatory funnel. The EtOAc layer was separated, washed with brine (2×5 mL), dried, and concentrated to afford additional 2-fluoro-3-iodo-4-methylbenzoic acid (1.6 g, LCMS >95% pure) as a tan solid. $^1\text{H NMR}$ (DMSO- d_6): δ 2.48 (s, 3H), 7.27 (d, $J = 7.9$ Hz, 1H), 7.75 (t, $J = 7.8$ Hz, 1H), 12.01 (br, 1H). MS (ESI, positive ion) m/z : 280.9 (M + 1).

2-Fluoro-3-iodo-4-methylbenzaldehyde (24). To a solution of 2-fluoro-3-iodo-4-methylbenzoic acid (2.0 g, 7.1 mmol) in anhydrous THF (10 mL) was added trimethyl borate (0.80 mL, 7.1 mmol) at room temperature. The resulting mixture was stirred at room temperature for 15 min, then cooled with an ice bath and treated with borane-dimethyl sulfide (6.4 mL of 2.0 M solution in THF, 12.8 mmol) slowly. The reaction mixture was stirred at room temperature for 4 h. MeOH (0.5 mL) was then added dropwise at room temperature. After being stirred for 30 min, the reaction mixture was concentrated in vacuo. The residue was diluted with EtOAc and washed with saturated aqueous solution of sodium bicarbonate followed by brine. The resulting organic solution was then dried over magnesium sulfate and concentrated under reduced pressure to give 2-fluoro-3-iodo-4-methylphenylmethanol (1.69 g, 89% yield) as an off-white amorphous solid, which was used without further purification. $^1\text{H NMR}$ (DMSO- d_6): δ 7.34 (t, $J = 7.6$ Hz, 1H), 7.16 (8.0 Hz, 1H), 5.27 (t, $J = 5.7$ Hz, 1H), 4.51 (d, $J = 5.7$ Hz, 2H), 2.40 (s, 3H).

A solution of the above-obtained (2-fluoro-3-iodo-4-methylphenyl)methanol (1.69 g, 6.35 mmol) in 50 mL of DCM at room temperature was treated with MnO_2 (5.57 g, 63.5 mmol), and the resulting mixture was stirred overnight. The mixture was filtered through a pad of Celite and eluted with DCM. The filtrate was concentrated. Purification was effected by flash chromatography on silica gel (15–35% EtOAc in hexanes) to provide the title compound (1.5 g, 89% yield) as an off-white solid. $^1\text{H NMR}$ (CDCl_3): δ 2.56 (s, 3H), 7.19 (d, $J = 8.0$ Hz, 1H), 7.74 (t, $J = 7.4$ Hz, 1H), 10.29 (s, 1H). MS (ESI, positive ion) m/z : 264.9 (M + 1).

(E)-2-Fluoro-3-iodo-4-methylbenzaldehyde Oxime (25). A solution of 2-fluoro-3-iodo-4-methylbenzaldehyde (1.26 g, 4.77 mmol) in EtOH (5 mL) at room temperature was treated with 5 mL of hydroxylamine (50% wt in water), and the reaction was allowed to continue for 3 h, when the crude LCMS indicated no remaining starting material. Volatiles were removed, and the residue was treated with 5 mL of water and extracted with EtOAc (3×15 mL). The combined EtOAc layers were dried and concentrated. Purification was effected by flash chromatography on silica gel (10–50% EtOAc in hexanes) to provide the title compound (1.13 g, 85% yield) as an off-white crystalline solid. $^1\text{H NMR}$ (CDCl_3): δ 2.49 (s, 3H), 7.06 (d, $J = 8.1$ Hz, 1H), 7.42 (br, 1H), 7.63 (t, $J = 7.6$ Hz, 1H), 8.34 (s, 1H). MS (ESI, positive ion) m/z : 280.0 (M + 1).

***N*-Cyclopropyl-2-fluoro-*N'*-hydroxy-3-iodo-4-methylbenzamide (26a).** To a solution of 2-fluoro-3-iodo-4-methylbenzaldehyde oxime (0.48 g, 1.7 mmol) in DMF (0.5 mL) was added *N*-chlorosuccinimide (83 mg, 0.62 mmol), and the mixture was heated at 55 °C for 5 min. The mixture was allowed to cool to <50 °C, and additional *N*-chlorosuccinimide (166 mg, 1.24 mmol) was added. Then the mixture was heated at 55 °C for 10 min. The reaction mixture was allowed to cool to room temperature, treated with 5 mL of water, and extracted with EtOAc (3×20 mL). The combined EtOAc layers were washed with 5 mL of brine, dried, and concentrated to afford the intermediate 2-fluoro-3-iodo-4-methylbenzoyl chloride oxime as a light-yellow amorphous solid, which was used without further purification. MS (ESI, positive ion) m/z : 314.3 (M + 1).

Cyclopropylamine (0.60 mL, 8.6 mmol) was added dropwise to an ice-cold solution of the above-obtained 2-fluoro-3-iodo-4-methylbenzoyl chloride oxime in anhydrous THF (2 mL). The reaction mixture was stirred at room temperature for 3 h, when

LCMS indicated the reaction to be completed. The volatiles were removed under reduced pressure. Purification was effected by flash chromatography on silica gel (25–60% EtOAc in hexanes) to provide the title compound (505 mg, 89% yield) as an amorphous off-white solid. $^1\text{H NMR}$ (CDCl_3): δ 7.23 (d, $J = 7.3$ Hz, 1H), 7.08 (d, $J = 7.9$ Hz, 1H), 5.60 (br, 1H), 2.51 (s, 3H), 2.43 (m, 1H), 0.40 (m, 4H). MS (ESI, positive ion) m/z : 335 ($M + 1$).

***N*-Cyclopropyl-7-iodo-6-methylbenzo[*d*]isoxazol-3-amine (27).** 1,8-Diazabicyclo [5.4.0]-7-undecene (0.25 mL, 1.65 mmol) was added to *N*-cyclopropyl-2-fluoro-*N'*-hydroxy-3-iodo-4-methylbenzamidinium (**26a**) (500 mg, 1.5 mmol) in anhydrous THF (2.0 mL) and NMP (0.5 mL), then heated in a microwave at 150 °C for 70 min. Volatiles were evaporated under reduced pressure. Purification was effected by flash chromatography on silica gel (25–75% EtOAc in hexanes) to provide the title compound (338 mg, 72% yield) as an off-white crystalline solid. $^1\text{H NMR}$ (CDCl_3): δ 0.70 (m, 2H), 0.86 (m, 2H), 2.57 (s, 3H), 2.83 (m, 1H), 4.65 (s, 1H), 7.08 (d, $J = 7.9$ Hz, 1H), 7.39 (d, $J = 7.8$ Hz, 1H). MS (ESI, positive ion) m/z : 315.0 ($M + 1$).

A similar procedure was used to prepare compounds **28** and **29**.

***N*-Ethyl-7-iodo-6-methylbenzo[*d*]isoxazol-3-amine (28).** $^1\text{H NMR}$ (CDCl_3): δ 1.34 (t, $J = 7.3$ Hz, 3H), 2.57 (s, 3H), 3.46 (m, 2H), 4.10 (br, 1H), 7.08 (d, $J = 8.0$ Hz, 1H), 7.29 (d, $J = 7.9$ Hz, 1H). MS (ESI, positive ion) m/z : 303 ($M + 1$).

7-Iodo-*N*,6-dimethylbenzo[*d*]isoxazol-3-amine (29). $^1\text{H NMR}$ (CDCl_3): δ 2.57 (s, 3H), 3.09 (s, 3H), 4.12 (br, 1H), 7.07 (d, $J = 7.9$ Hz, 1H), 7.29 (d, $J = 7.9$ Hz, 1H). MS (ESI, positive ion) m/z : 289 ($M + 1$).

7-Iodo-6-methylbenzo[*d*]isoxazol-3-amine (30). To a 250 mL three-necked round-bottomed flask equipped with a mechanical stirrer and under nitrogen containing anhydrous DMF (100 mL) was added acetoxyhydroxamic acid (4.65 g, 62 mmol). After a clear solution was obtained, potassium *tert*-butoxide (6.94 g, 62 mmol) was added to the mixture. The cloudy white mixture was allowed to stir for 30 min. 2-Fluoro-3-iodo-4-methylbenzimidazole (**22**) (8.0 g, 31 mmol) was added, and the reaction mixture was allowed to stir at room temperature for 6 h. Additional reagents of acetoxyhydroxamic acid (1.16 g, 15.5 mmol) and potassium *tert*-butoxide (1.74 g, 15.5 mmol) were added to the reaction mixture, and the stirring was continued for 12 h. The reaction mixture was distilled under reduced pressure to remove most of the DMF, and the remaining residue was partitioned between EtOAc (250 mL) and saturated ammonium chloride solution (50 mL). The water layer was washed with EtOAc (2 \times 100 mL). The combined organic layers were washed with brine (50 mL), dried over MgSO_4 , and evaporated under reduced pressure. Purification was effected by flash chromatography on silica gel (20–70% EtOAc in hexanes) to provide the title compound (5.8 g, 69% yield) as an off-white crystalline solid. $^1\text{H NMR}$ (CDCl_3): δ 2.59 (s, 3H), 4.24 (br, 2H), 7.13 (d, $J = 8.1$ Hz, 1H), 7.35 (d, $J = 8.1$ Hz, 1H). MS (ESI, positive ion) m/z : 275.0 ($M + 1$).

***N*-(7-Iodo-6-methylbenzo[*d*]isoxazol-3-yl)acetamide (31).** To a mixture of 7-iodo-6-methylbenzo[*d*]isoxazol-3-amine (0.30 g, 1.09 mmol) and cesium carbonate (0.43 g, 1.31 mmol) in DCM (10.0 mL) was added acetyl chloride (95 mg, 1.20 mmol). After the mixture was stirred at room temperature for 20 min, it was treated with 5.0 mL of water and stirred for 10 min. The resulting mixture was extracted with EtOAc (3 \times 30 mL). The combined organic phases were washed with saturated aqueous solution of sodium bicarbonate followed by brine. The resulting organic solution was dried over magnesium sulfate and concentrated under reduced pressure to give the title compound (0.32 g, 92% yield) as an off-white amorphous solid. $^1\text{H NMR}$ (CDCl_3): δ 2.02 (s, 3H), 2.46 (s, 3H), 7.13 (d, $J = 8.0$ Hz, 1H), 7.36 (d, $J = 8.0$ Hz, 1H), 8.00 (br, 1H). MS (ESI, positive ion) m/z : 317.0 ($M + 1$).

Alternative Procedure for the Synthesis of 7-Iodo-*N*,6-dimethylbenzo[*d*]isoxazol-3-amine (29). At room temperature, trifluoroacetic anhydride (0.63 mL, 4.45 mmol) was added to a solution of 7-iodo-6-methylbenzo[*d*]isoxazol-3-amine **30** (1.11 g, 4.05 mmol) in 10 mL of DCM. After the mixture was stirred for 6 h, the volatiles were removed under reduced pressure to provide

2,2,2-trifluoro-*N*-(7-iodo-6-methylbenzo[*d*]isoxazol-3-yl)acetamide as an off-white solid, which was used prior to further purification. MS (ESI, positive ion) m/z : 370.9 ($M + 1$).

To the above-obtained 2,2,2-trifluoro-*N*-(7-iodo-6-methylbenzo[*d*]isoxazol-3-yl)acetamide in acetone (5.0 mL) at room temperature were added dimethyl sulfate (766 mg, 6.07 mmol) and potassium carbonate (1.40 g, 10.12 mmol). The mixture was heated at 50 °C in an oil bath for 5 h, then cooled to room temperature, filtered through a pad of Celite, and rinsed with additional acetone (2 \times 5 mL). The filtrate was concentrated to dryness to provide 2,2,2-trifluoro-*N*-(7-iodo-6-methylbenzo[*d*]isoxazol-3-yl)-*N*-methylacetamide, which was used prior to further purification. MS (ESI, positive ion) m/z : 385.0 ($M + 1$).

At room temperature, the above-obtained 2,2,2-trifluoro-*N*-(7-iodo-6-methylbenzo[*d*]isoxazol-3-yl)-*N*-methylacetamide was dissolved in 10 mL of MeOH and treated with 10 mL of 1 N NaOH. After the mixture was stirred at room temperature for 2 h, the solvents were removed under reduced pressure. The residue was treated with saturated ammonium chloride solution (20 mL) and extracted with EtOAc (3 \times 50 mL). The combined organic layers were dried over Na_2SO_4 and concentrated. Purification was effected by flash chromatography on silica gel (25–65% EtOAc in hexanes) to provide 7-iodo-*N*,6-dimethylbenzo[*d*]isoxazol-3-amine (794 mg, 68% yield) as an off-white crystalline solid. $^1\text{H NMR}$ (CDCl_3): δ 2.57 (s, 3H), 3.09 (s, 3H), 4.12 (br, 1H), 7.07 (d, $J = 7.9$ Hz, 1H), 7.29 (d, $J = 7.9$ Hz, 1H). MS (ESI, positive ion) m/z : 289.0 ($M + 1$).

(4-Chloro-2-fluorobenzoyloxy)(*tert*-butyl)dimethylsilane (33).

To a solution of (4-chloro-2-fluorophenyl)methanol (4.60 g, 28.6 mmol) in DCM (100 mL) was added imidazole (1.95 g, 28.6 mmol) and *tert*-butylchlorodimethylsilane (4.32 g, 28.6 mmol) at room temperature. The reaction mixture was stirred for 12 h at room temperature. The white precipitate was removed by filtration, and the filtrate was washed with 10% HCl. The separated aqueous phase was extracted with DCM (2 \times 40 mL). The combined organic phases were washed with saturated aqueous solution of sodium bicarbonate followed by brine. The resulting organic solution was dried over magnesium sulfate and concentrated under reduced pressure. Purification was effected by flash chromatography on silica gel (eluted with hexanes) to give the title compound (6.64 g, 84.3% yield) as a colorless oil. $^1\text{H NMR}$ (CDCl_3): δ 0.00 (s, 6H), 0.81 (s, 9H), 4.64 (s, 2H), 6.91 (dd, $J = 9.9$, 1.8 Hz, 1H), 7.01 (d, $J = 8.3$ Hz, 1H), 7.31 (t, $J = 8.1$ Hz, 1H).

(4-Chloro-2-fluoro-3-iodobenzoyloxy)(*tert*-butyl)dimethylsilane (34).

To a solution of diisopropylamine (3.09 mL, 21.8 mmol) in THF (60 mL) under N_2 at 0 °C was slowly added *n*-butyllithium (8.72 mL of 2.5 M solution in hexanes, 21.8 mmol) over 5 min. After being stirred at 0 °C for 20 min, the reaction mixture was cooled to -78 °C, and a solution of silyl ether **33** (5.00 g, 18.2 mmol) in 15 mL of THF was added slowly over 5 min. After the mixture was stirred for 2 h at -78 °C, a solution of iodine (5.54 g, 21.8 mmol) in 25 mL of THF was added slowly over 10 min. The reaction mixture was allowed to stir for 20 min at -78 °C and warmed to room temperature in 20 min. The reaction was quenched with saturated sodium thiosulfate solution and extracted with Et_2O (2 \times 60 mL). The combined organic phases were washed with saturated sodium bicarbonate and brine. The resulting organic solution was then dried over magnesium sulfate and concentrated under reduced pressure. Purification was effected by flash chromatography on silica gel (5–10% DCM in hexanes) to give the title compound (6.11 g, 84% yield) as a colorless oil. $^1\text{H NMR}$ (CDCl_3): δ 0.01 (s, 6H), 0.80 (s, 9H), 4.65 (s, 2H), 7.17 (d, $J = 7.1$ Hz, 1H), 7.30 (t, $J = 7.5$ Hz, 1H).

(4-Chloro-2-fluoro-3-iodophenyl)methanol (35). To a solution of (4-chloro-2-fluoro-3-iodobenzoyloxy)(*tert*-butyl)dimethylsilane **34** (6.64 g, 16.6 mmol) in THF (60 mL) was added tetrabutylammonium fluoride (19.9 mL of 1.0 M solution in THF, 19.9 mmol). The reaction solution was stirred at room temperature for 1 h. The volatiles were removed via vacuum. The brown residue was diluted with 150 mL of Et_2O and washed with saturated aqueous solution of sodium bicarbonate and brine. The resulting organic solution

was dried over magnesium sulfate and concentrated under reduced pressure. Purification was effected by flash chromatography on silica gel (eluted with DCM) to give the title compound (4.60 g, 97% yield) as a colorless oil. $^1\text{H NMR}$ (CDCl_3) δ 1.90 (t, $J = 5.7$ Hz, 1H), 4.66 (d, $J = 5.7$ Hz, 2H), 7.16–7.32 (m, 2H). MS (ESI, positive ion) m/z : 289.0 ($M + 1$).

6-Chloro-7-iodo-*N*-methylbenzo[*d*]isoxazol-3-amine (36). Following the procedure described for the synthesis of compound 27, using (4-chloro-2-fluoro-3-iodophenyl)methanol (35), the title compound was obtained (43% overall yield for five steps) as an off-white solid. $^1\text{H NMR}$ (CDCl_3): δ 7.34 (d, $J = 8.4$ Hz, 1H), 7.28 (d, $J = 8.4$ Hz, 1H), 4.16 (br, 1H), 3.08 (d, $J = 4.7$ Hz, 3H). MS (ESI, positive ion) m/z : 309 ($M + 1$).

6-Chloro-7-iodo-*N*-isopropylbenzo[*d*]isoxazol-3-amine (37). Following the procedure described for the synthesis of compound 27, using (4-chloro-2-fluoro-3-iodophenyl)methanol (35), the title compound was obtained (41% overall yield for five steps) as an off-white solid. $^1\text{H NMR}$ (CDCl_3): δ 7.34 (d, $J = 8.4$ Hz, 1H), 7.28 (d, $J = 8.4$ Hz, 1H), 4.01 (br, 1H), 3.97 (m, 1H), 1.34 (d, $J = 6.2$ Hz, 6H). MS (ESI, positive ion) m/z : 338 ($M + 1$).

7-Iodo-6-methyl-1*H*-indazol-3-amine (38). A solution of 2-fluoro-3-iodo-4-methylbenzonitrile (200 mg, 0.77 mmol) in hydrazine hydrate (0.48 mL, 1.53 mmol) in 0.5 mL of THF was heated at 80 °C in an oil bath for 16 h. The mixture was cooled to room temperature and partitioned between EtOAc and water. The EtOAc layer was separated, dried, and concentrated. Purification was effected by flash chromatography on silica gel (50–80% EtOAc in hexanes) to provide the title compound (189 mg, 90% yield) as an off-white amorphous solid. $^1\text{H NMR}$ (CDCl_3): δ 8.80 (br, 1H), 7.41 (d, $J = 8.0$ Hz, 1H), 6.96 (d, $J = 8.0$ Hz, 1H), 4.18 (br, 2H), 2.55 (s, 3H). MS (ESI, positive ion) m/z : 274.0 ($M + 1$).

7-Iodo-6-methylbenzo[*d*]isothiazol-3-amine (39). A mixture of 2-fluoro-3-iodo-4-methylbenzonitrile (130 mg, 0.50 mmol), sulfur (16 mg, 0.50 mmol), and ammonium hydroxide (28–30%, 0.25 mL) in 2-methoxyethanol (1.5 mL) was heated in an oil bath at 135 °C for 12 h. Volatiles were removed under reduced pressure. Purification was effected by flash chromatography on silica gel (25–50% EtOAc in hexanes) to provide the title compound (45 mg, 31% yield) as a yellow crystalline solid. $^1\text{H NMR}$ ($\text{DMSO-}d_6$): δ 7.65 (d, $J = 8.1$ Hz, 1H), 7.19 (d, $J = 8.0$ Hz, 1H), 3.35 (br, 2H), 2.51 (s, 3H). MS (ESI, positive ion) m/z : 291.0 ($M + 1$).

***N*-Cyclopropyl-6-methyl-7-(1-((*S*)-3-methylmorpholino)phthalazin-6-yl)benzo[*d*]isoxazol-3-amine (3a).** A mixture of (*S*)-1-(3-methylmorpholino)phthalazin-6-ylboronic acid 9 (0.11 g, 0.41 mmol), *N*-cyclopropyl-7-iodo-6-methylbenzo[*d*]isoxazol-3-amine 27 (0.10 g, 0.32 mmol), tetrakis(triphenylphosphine)palladium(0) (18 mg, 0.016 mmol) in 2.0 mL of 1,4-dioxane, and sodium carbonate (0.32 mL of 2 N solution) in a sealed glass tube was heated in a Personal Chemistry microwave at 130 °C for 20 min. The mixture was diluted with EtOAc (30 mL) and washed with 1 N NaOH (5 mL) followed by brine. The organic phase was dried over magnesium sulfate and concentrated under reduced pressure. Purification was effected by flash chromatography on silica gel (eluted with 80–100% EtOAc in hexanes) to give the title compound (59 mg, 45% yield) as a yellow amorphous solid. $^1\text{H NMR}$ (CDCl_3): δ 0.79–0.91 (m, 3H), 1.16–1.31 (m, 4H), 2.41 (s, 3H), 2.81 (m, 1H), 3.43 (m, 1H), 3.60 (m, 2H), 3.91–4.15 (m, 4H), 5.03 (s, 1H), 7.21 (d, $J = 8.0$ Hz, 1H), 7.56 (d, $J = 8.0$ Hz, 1H), 7.91 (d, $J = 8.4$ Hz, 1H), 8.00 (s, 1H), 8.20 (d, $J = 8.4$ Hz, 1H), 9.23 (s, 1H). MS (ESI, positive ion) m/z : 416 ($M + 1$). Anal. ($\text{C}_{24}\text{H}_{25}\text{N}_5\text{O}_2$) C, H, N.

Similar procedures were used to prepare compounds 3b–n, 40, and 41.

***N*-Ethyl-6-methyl-7-(1-((*S*)-3-methylmorpholino)phthalazin-6-yl)benzo[*d*]isoxazol-3-amine (3b).** $^1\text{H NMR}$ (CDCl_3): δ 1.27 (d, $J = 6.6$ Hz, 3H), 1.36 (t, $J = 7.0$ Hz, 3H), 2.42 (s, 3H), 3.48 (m, 3H), 3.70 (m, 2H), 3.91–4.15 (m, 5H), 7.23 (d, $J = 8.2$ Hz, 1H), 7.43 (d, $J = 8.0$ Hz, 1H), 7.92 (d, $J = 8.4$ Hz, 1H), 8.01 (s, 1H), 8.20 (d, $J = 8.4$ Hz, 1H), 9.28 (s, 1H). MS (ESI, positive ion) m/z : 404 ($M + 1$). Anal. ($\text{C}_{23}\text{H}_{25}\text{N}_5\text{O}_2$) C, H, N.

***N*,6-Dimethyl-7-(1-((*S*)-3-methylmorpholino)phthalazin-6-yl)benzo[*d*]isoxazol-3-amine (3c).** $^1\text{H NMR}$ (CDCl_3): δ 1.25 (d, $J = 6.4$ Hz, 3H), 2.41 (s, 3H), 3.10 (d, $J = 5.2$ Hz, 3H), 3.43 (m, 1H), 3.70 (m, 2H), 3.91–4.15 (m, 4H), 4.50 (m, 1H), 7.21 (d, $J = 8.1$ Hz, 1H), 7.43 (d, $J = 8.0$ Hz, 1H), 7.92 (d, $J = 8.4$ Hz, 1H), 7.99 (s, 1H), 8.20 (d, $J = 8.4$ Hz, 1H), 9.23 (s, 1H). MS (ESI, positive ion) m/z : 390 ($M + 1$). Anal. ($\text{C}_{22}\text{H}_{23}\text{N}_5\text{O}_2$) C, H, N.

6-Methyl-7-(1-((*S*)-3-methylmorpholino)phthalazin-6-yl)benzo[*d*]isoxazol-3-amine (3d). $^1\text{H NMR}$ (CDCl_3): δ 1.24 (d, $J = 6.4$ Hz, 3H), 2.43 (s, 3H), 3.43 (m, 1H), 3.71 (m, 2H), 3.91–4.15 (m, 5H), 4.42 (s, 1H), 7.27 (d, $J = 8.3$ Hz, 1H), 7.49 (d, $J = 8.3$ Hz, 1H), 7.91 (d, $J = 8.4$ Hz, 1H), 7.98 (s, 1H), 8.22 (d, $J = 8.4$ Hz, 1H), 9.25 (s, 1H). MS (ESI, positive ion) m/z : 376 ($M + 1$).

***N*-(6-Methyl-7-(1-((*S*)-3-methylmorpholino)phthalazin-6-yl)benzo[*d*]isoxazol-3-yl)acetamide (3e).** $^1\text{H NMR}$ (CDCl_3) δ 1.25 (d, $J = 6.4$ Hz, 3H), 2.03 (s, 3H), 2.43 (s, 3H), 3.45 (m, 1H), 3.71 (m, 2H), 3.91–4.13 (m, 4H), 4.42 (s, 1H), 7.27 (d, $J = 8.3$ Hz, 1H), 7.49 (d, $J = 8.3$ Hz, 1H), 7.91 (d, $J = 8.4$ Hz, 1H), 7.98 (s, 1H), 8.22 (m, 1H), 9.25 (s, 1H). MS (ESI, positive ion) m/z : 418 ($M + 1$). HRMS (EI) m/z calcd for $\text{C}_{23}\text{H}_{24}\text{N}_5\text{O}_3$ [$M + \text{H}$] $^+$: 418.1879; found, 418.1897.

1-((*S*)-4-(6-(3-(Cyclopropylamino)-6-methylbenzo[*d*]isoxazol-7-yl)phthalazin-1-yl)-3-methylpiperazin-1-yl)ethanone (3f). $^1\text{H NMR}$ (CDCl_3) δ 0.73 (m, 2H), 0.88 (m, 2H), 1.24 (m, 3H), 2.19 (s, 3H), 2.43 (s, 3H), 2.86 (m, 1H), 3.54–3.86 (m, 4H), 4.13 (m, 3H), 4.75 (d, $J = 3.7$ Hz, 1H), 7.22 (m, 1H), 7.53 (m, 1H), 8.01 (m, 2H), 8.17 (m, 1H), 9.24 (s, 1H). MS (ESI, positive ion) m/z : 457.0 ($M + 1$).

6-(3-(Cyclopropylamino)-6-methylbenzo[*d*]isoxazol-7-yl)-*N*,*N*-dimethylphthalazin-1-amine (3g). $^1\text{H NMR}$ (CDCl_3) δ 0.72 (m, 2H), 0.86 (m, 2H), 1.41 (d, $J = 6.4$ Hz, 6H), 2.39 (s, 3H), 2.86 (m, 1H), 4.71 (m, 1H), 4.74 (br, 1H), 4.95 (br, 1H), 7.20 (d, $J = 8.2$ Hz, 1H), 7.50 (d, $J = 8.0$ Hz, 1H), 7.85 (m, 3H), 8.94 (s, 1H). MS (ESI, positive ion) m/z : 373.8 ($M + 1$).

6-Chloro-*N*-cyclopropyl-7-(1-((*S*)-3-methylmorpholino)phthalazin-6-yl)benzo[*d*]isoxazol-3-amine (3h). $^1\text{H NMR}$ (CDCl_3) δ 9.21–9.30 (s, 1H), 8.22 (d, $J = 8.6$ Hz, 1H), 8.14 (s, 1H), 8.03 (d, $J = 8.4$ Hz, 1H), 7.51 (d, $J = 8.4$ Hz, 1H), 7.41 (d, $J = 8.4$ Hz, 1H), 4.63 (s, 1H), 3.92–4.16 (m, 4H), 3.64–3.74 (m, 2H), 3.44 (m, 1H), 3.11 (d, $J = 4.7$ Hz, 3H), 1.25 (d, $J = 6.3$ Hz, 3H). MS (ESI, positive ion) m/z : 410.2 ($M + 1$). HRMS (EI) m/z calcd for $\text{C}_{21}\text{H}_{21}\text{ClN}_5\text{O}_2$ [$M + \text{H}$] $^+$: 410.1384; found, 410.1399.

6-Chloro-*N*-isopropyl-7-(1-((*S*)-3-methylmorpholino)phthalazin-6-yl)benzo[*d*]isoxazol-3-amine (3i). $^1\text{H NMR}$ (CDCl_3): δ 9.25 (s, 1H), 8.21 (d, $J = 8.6$ Hz, 1H), 8.14 (s, 1H), 8.03 (dd, $J = 8.6, 1.6$ Hz, 1H), 7.39–7.56 (m, 3H), 4.33 (d, $J = 7.4$ Hz, 1H), 3.93–4.14 (m, 4H), 3.66–3.75 (m, 2H), 3.42 (m, 1H), 1.36 (d, $J = 2.0$ Hz, 6H), 1.24 (d, $J = 4.0$ Hz, 3H). MS (ESI, positive ion) m/z : 438.3 ($M + 1$). HRMS (EI) m/z calcd for $\text{C}_{23}\text{H}_{25}\text{ClN}_5\text{O}_2$ [$M + \text{H}$] $^+$: 438.1691; found, 438.1705.

***N*,6-Dimethyl-7-(1-((*R*)-3-methylmorpholino)phthalazin-6-yl)benzo[*d*]isoxazol-3-amine (3j).** $^1\text{H NMR}$ (CDCl_3): δ 1.25 (d, $J = 6.4$ Hz, 3H), 2.41 (s, 3H), 3.10 (d, $J = 5.2$ Hz, 3H), 3.43 (m, 1H), 3.70 (m, 2H), 3.91–4.15 (m, 4H), 4.50 (m, 1H), 7.21 (d, $J = 8.1$ Hz, 1H), 7.43 (d, $J = 8.0$ Hz, 1H), 7.92 (d, $J = 8.4$ Hz, 1H), 7.99 (s, 1H), 8.20 (d, $J = 8.4$ Hz, 1H), 9.23 (s, 1H). MS (ESI, positive ion) m/z : 390 ($M + 1$).

***N*-Isopropyl-6-(6-methyl-3-(methylamino)benzo[*d*]isoxazol-7-yl)phthalazin-1-amine (3k).** $^1\text{H NMR}$ (CDCl_3): δ 1.41 (d, $J = 6.3$ Hz, 6H), 2.38 (s, 3H), 3.11 (d, $J = 5.3$ Hz, 3H), 4.27 (br, 1H), 4.70 (m, 1H), 4.95 (br, 1H), 7.21 (d, $J = 8.1$ Hz, 1H), 7.41 (d, $J = 8.0$ Hz, 1H), 7.86 (m, 3H), 8.94 (s, 1H). MS (ESI, positive ion) m/z : 347.8 ($M + 1$).

***N*-(*S*)-*sec*-Butyl-6-(6-methyl-3-(methylamino)benzo[*d*]isoxazol-7-yl)phthalazin-1-amine (3l).** $^1\text{H NMR}$ (CDCl_3): δ 1.05 (m, 3H), 1.38 (m, 3H), 1.60–1.80 (m, 2H), 2.43 (s, 3H), 3.22 (s, 3H), 4.28 (br, 1H), 4.58 (m, 1H), 4.96 (br, 1H), 7.20 (d, $J = 7.6$ Hz, 1H), 7.28 (m, 1H), 7.41 (d, $J = 7.9$ Hz, 1H), 7.86 (m, 2H), 8.93 (s, 1H). MS (ESI, positive ion) m/z : 362 ($M + 1$).

7-(1-Isopropoxyphthalazin-6-yl)-N,6-dimethylbenzo[d]isoxazol-3-amine (3m). $^1\text{H NMR}$ (methanol- d_4) δ : 1.56 (d, $J = 6.02$ Hz, 6H), 2.40 (s, 3H), 2.98 (s, 3H), 5.72 (t, $J = 6.02$ Hz, 1H), 7.30 (d, $J = 8.53$ Hz, 1H), 7.67 (d, $J = 8.03$ Hz, 1H), 8.03 (d, $J = 8.03$ Hz, 1H), 8.14 (s, 1H), 8.38 (d, $J = 8.53$ Hz, 1H), 9.25 (s, 1H). MS (ESI, positive ion) m/z : 348.8 ($M + 1$). Anal. ($\text{C}_{20}\text{H}_{20}\text{N}_4\text{O}_2$) C, H, N.

7-(1-Isopropylphthalazin-6-yl)-N,6-dimethylbenzo[d]isoxazol-3-amine (3n). $^1\text{H NMR}$ (CDCl_3): δ 1.59 (d, $J = 6.85$ Hz, 6H), 2.41 (s, 3H), 3.11 (d, $J = 5.09$ Hz, 3H), 3.89–4.04 (m, 1H), 4.27 (br, 1H), 7.23 (d, $J = 8.22$ Hz, 1H), 7.43 (d, $J = 8.02$ Hz, 1H), 7.98 (d, $J = 8.61$ Hz, 1H), 8.03 (s, 1H), 8.27 (d, $J = 8.41$ Hz, 1H), 9.43 (s, 1H). MS (ESI, positive ion) m/z : 333.2 ($M + 1$). HRMS (EI) m/z calcd for $\text{C}_{20}\text{H}_{21}\text{N}_4\text{O}$ [$M + \text{H}$] $^+$: 333.1715; found, 333.1729.

6-Methyl-7-(1-((S)-3-methylmorpholino)phthalazin-6-yl)-1H-indazol-3-amine (40). $^1\text{H NMR}$ (CDCl_3): δ 1.25 (d, $J = 6.3$ Hz, 3H), 2.33 (s, 3H), 3.41 (m, 2H), 3.49 (s, 1H), 3.70 (m, 3H), 3.90–4.11 (m, 4H), 7.08 (d, $J = 8.3$ Hz, 1H), 7.51 (d, $J = 8.2$ Hz, 1H), 7.87 (m, 1H), 7.94 (s, 1H), 8.21 (d, $J = 8.5$ Hz, 1H), 9.21 (s, 1H). MS (ESI, positive ion) m/z : 374.9 ($M + 1$).

6-Methyl-7-(1-((S)-3-methylmorpholino)phthalazin-6-yl)benzo[d]isothiazol-3-amine (41). $^1\text{H NMR}$ (CDCl_3): δ 1.27 (d, $J = 6.3$ Hz, 3H), 2.37 (s, 3H), 3.43 (m, 1H), 3.70 (m, 2H), 3.90–4.13 (m, 4H), 4.93 (br, 2H), 7.41 (d, $J = 8.3$ Hz, 1H), 7.66 (d, $J = 8.0$ Hz, 1H), 7.88 (d, $J = 8.6$ Hz, 1H), 7.96 (s, 1H), 8.23 (d, $J = 8.5$ Hz, 1H), 9.25 (s, 1H). MS (ESI, positive ion) m/z : 392.2 ($M + 1$). Anal. ($\text{C}_{21}\text{H}_{21}\text{N}_5\text{OS}$) C, H, N.

Biological Methods. p38 α MAP Kinase in Vitro Assay. The p38 α kinase reaction was carried out in a polypropylene 96-well black round-bottomed assay plate in a total volume of 30 μL of kinase reaction buffer (50 mM Tris, pH 7.5, 5 mM MgCl_2 , 0.1 mg/mL BSA, 100 μM Na_2VO_4 , and 0.5 mM DTT). Recombinant activated human p38 enzyme (1 nM) was mixed with 50 μM ATP and 100 nM GST-ATF2-Avitag, in the presence or absence of inhibitor. The mixture was allowed to incubate for 1 h at room temperature. The kinase reaction was terminated, and phospho-ATF2 was revealed by addition of 30 μL of HTRF detection buffer (100 mM HEPES, pH 7.5, 100 mM NaCl, 0.1% BSA, 0.05% Tween-20, and 10 mM EDTA) supplemented with 0.1 nM Eu-anti-pTP and 4 nM SA-APC. After 1 h of incubation at room temperature, the assay plate was read in a Discovery plate reader (Perkin-Elmer). The wells were excited with coherent 320 nm light, and the ratio of delayed (50 ms after excitation) emissions at 620 nm (native europium fluorescence) and 665 nm (europium fluorescence transferred to allophycocyanin (an index of substrate phosphorylation)) was determined (reference, Park, Y. W.; Cummings, R. T.; Wu, L. Homogeneous Proximity Tyrosine Kinase Assays: Scintillation Proximity Assay versus Homogeneous Time-Resolved Fluorescence. *Anal. Biochem.* **1999**, *269*, 94–104). The proportion of substrate phosphorylated in the kinase reaction in the presence of compound compared with that phosphorylated in the presence of DMSO vehicle alone (HI control) was calculated using the following formula: % control (POC) = (compd – average LO)/(average HI – average LO) \times 100. Data (consisting of POC and inhibitor concentration in μM) were fitted to a four-parameter equation $y = A + [(B - A)/(1 + (x/C)^D)]$, where A is the minimum y (POC) value, B is the maximum y (POC), C is the x (compound concentration) at the point of inflection, and D is the slope factor, using a Levenburg–Marquardt nonlinear regression algorithm. The inhibition constant (K_i) of the inhibitor was estimated from the IC_{50} (compound concentration at the point of inflection, C) using the Cheng–Prusoff equation: $K_i = \text{IC}_{50} / (1 + S/K_m)$, where S is the ATP substrate concentration and K_m is the Michaelis constant for ATP as determined experimentally.

ATP Competitive Assay. The method for this experiment was the same as for the p38 α enzyme assay except that the ATP concentration was varied in the range of 1.3 μM to 5 mM. For kinetic studies, the concentrations of the inhibitor (**3c**) were 0 (DMSO solution), 6, 9, 13, and 19 nM.

LPS-Induced TNF α Production in THP-1 Cells. THP1 cells were resuspended in fresh THP1 media (RPMI 1640, 10% heat-inactivated FBS, 1 \times PGS, 1 \times NEAA, plus 30 μM βME) at a concentration of 1.5×10^6 cells/mL. One hundred microliters of cells per well were plated in a flat bottom polystyrene 96-well tissue culture plate. Then 200 $\mu\text{g}/\text{mL}$ of bacterial LPS (Sigma) was prepared in THP1 media and transferred to the first 11 columns of a 96-well polypropylene plate. Column 12 contained only THP1 media for the LO control. Compounds were dissolved in 100% DMSO and serially diluted 3-fold in a polypropylene 96-well microtiter plate (drug plate). Columns 6 and 12 were reserved as controls (HI control and LO control, respectively) and contained only DMSO. An amount of 1 μL of inhibitor compound from the drug plate followed by 10 μL of LPS was transferred to the cell plate. The treated cells were induced to synthesize and secrete TNF α in a 37 $^\circ\text{C}$ humidified incubator with 5% CO_2 for 3 h. TNF α production was determined by transferring 50 μL of conditioned media to a 96-well small spot TNF α plate (MSD, Meso Scale Discovery) containing 100 μL of 2 \times Read Buffer P supplemented with an anti-TNF α polyclonal Ab labeled with ruthenium (MSD, Sulfo-TAG–NHS ester). After overnight incubation at room temperature with shaking, the reaction was read on the Sector Imager 6000 (MSD). A low voltage was applied to the ruthenylated TNF α immune complexes, which in the presence of TPA (the active component in the ECL reaction buffer, Read Buffer P) resulted in a cyclical redox reaction generating light at 620 nm. The amount of secreted TNF α in the presence of compound compared with that in the presence of DMSO vehicle alone (HI control) was calculated using the following formula: % control (POC) = (compd – average LO)/(average HI – average LO) \times 100.

TNF-Challenged IL-8 Production in Human Whole Blood Cells. Whole blood was drawn from healthy, nonmedicated volunteers into sodium heparin tubes. An amount of 100 μL of blood was then plated into 96 well tissue culture plates (BD). Ten point compound titrations were added to the blood and incubated for 1 h at 37 $^\circ\text{C}$ with 5% CO_2 . TNF α (Amgen) with a final concentration of 1 nM was then added to the blood and incubated overnight (16–18 h) at 37 $^\circ\text{C}$ with 5% CO_2 . Plasma was harvested, and cytokines (IL8) were measured by MSD (Meso Scale Discovery) ECL based antibody sandwich assay. All reagents were prepared in RPMI 1640, 10% v/v human serum AB (Gemini Bio-Products), 1 \times Pen/Strep/Glu. Final concentration of human whole blood was 50%. Data were analyzed using XLfit/Activity Base software package (IDBS).

CYP3A4 IC_{50} in Human Liver Microsomes. Midazolam 1'-hydroxylation was used to monitor the CYP3A4 activity. Inhibitor (0.41–100 μM) was co-incubated with midazolam (5 μM) in the presence of human liver microsomes (0.1 mg/mL) and NADPH (1 mM) at 37 $^\circ\text{C}$ for 5 min. Incubation containing no inhibitor was used as solvent control. At the end of the incubation, the reaction was terminated by the addition of 0.05% formic acid in acetonitrile. The concentration of 1'-hydroxymidazolam was determined by LCMS analysis. The inhibition of CYP3A4 activity was assessed by comparing the amount of 1'-hydroxymidazolam formed in presence of varying concentrations of inhibitor to the amount of 1'-hydroxymidazolam formed in the solvent control. The IC_{50} transit values were calculated by Excel-fit, version 4.1.1. In each study, a CYP3A4 potent and specific inhibitor, ketoconazole (0.037 μM), was used as positive control.

Acknowledgment. We thank Dr. Randy Jensen for providing 2D-NOESY NMR analyses.

Supporting Information Available: X-ray data of cocrystal of **1** in p38 α protein and HPLC purity (at two different conditions) or combustion analysis data for each biological testing compound. This material is available free of charge via the Internet at <http://pubs.acs.org>.

References

- (1) (a) O'Keefe, S. J.; Mudgett, J. S.; Cupo, S.; Parsons, J. N.; Chartrain, N. A.; Fitzgerald, C.; Chen, S.-L.; Lowitz, K.; Rasa, C.; Visco, D.; Luell, S.; Carballo-Jane, E.; Owens, K.; Zaller, D. M. Chemical Genetics Define the Roles of p38 α and p38 β in Acute and Chronic Inflammation. *J. Biol. Chem.* **2007**, *282*, 34663–34671. (b) Lee, J. C.; Newton, R.; Holden, N. Inhibitors of p38 Mitogen-Activated Protein Kinase Potential as Anti-Inflammatory Agents in Asthma. *BioDrugs* **2003**, *17*, 113–129. (c) Adams, J. L.; Badger, A. M.; Kumar, S.; Lee, J. C. p38 MAP Kinase: Molecular Target for the Inhibition of Pro-Inflammatory Cytokines. *Prog. Med. Chem.* **2001**, *38*, 1–60. (d) Lee, J. C.; Laydon, J. T.; McDonnell, P. C.; Gallagher, T. F.; Kumar, S.; Green, D.; McNulty, D.; Blumenthal, M. J.; Keys, J. R.; Land Vatter, S. W.; Strickler, J. E.; McLaughlin, M. M.; Siemens, I. R.; Fisher, S. M.; Livi, G. P.; White, J. R.; Adams, J. L.; Young, P. R. A Protein Kinase Involved in the Regulation of Inflammatory Cytokine Biosynthesis. *Nature* **1994**, *372*, 739–746.
- (2) (a) Foster, M. L.; Halley, F.; Souness, J. E. Potential of p38 Inhibitors in the Treatment of Rheumatoid Arthritis. *Drug News Perspect.* **2000**, *13*, 488–497. (b) Feldmann, M.; Brennan, F. M.; Maini, R. N. Role of Cytokines in Rheumatoid Arthritis. *Annu. Rev. Immunol.* **1996**, *14*, 397–440. (c) Tracey, K. J.; Cerami, A. *Annu. Rev. Cell Biol.* **1993**, *9*, 317–343.
- (3) (a) Goldsmith, D. R.; Wagstaff, A. J. Spotlight on Etanercept in Plaque Psoriasis and Psoriatic Arthritis. *BioDrugs* **2005**, *19* (6), 401–403. (b) Feldman, S. R.; Gordon, K. B.; Bala, M.; Evans, R.; Li, S.; Dooley, L. T.; Guzzo, C.; Patel, K.; Menter, A.; Gottlieb, A. B. Infliximab Treatment Results in Significant Improvement in the Quality of Life of Patients with Severe Psoriasis: A Double-Blind Placebo-Controlled Trial. *Br. J. Dermatol.* **2005**, *152* (5), 954–960. (c) Moreland, L. W. Soluble Tumor Necrosis Factor Receptor (p75) Fusion Protein (ENBREL) as a Therapy for Rheumatoid Arthritis. *Rheum. Dis. Clin. North Am.* **1998**, *24* (3), 579–591. (d) Bang, L. M.; Keating, G. M. Adalimumab: A Review of Its Use in Rheumatoid Arthritis. *BioDrugs* **2004**, *18* (2), 121–139.
- (4) (a) Graneto, M. J.; Kurumbail, R. G.; Vazquez, M. L.; Shieh, H.-S.; Pawlitz, J. L.; Williams, J. M.; Stallings, W. C.; Geng, L.; Naraian, A. S.; Koszyk, F. J.; Stealey, M. A.; Xu, X. D.; Weier, R. M.; Hanson, G. J.; Mourey, R. J.; Compton, R. P.; Minch, S. J.; Anderson, G. D.; Monahan, J. B.; Devraj, R. Synthesis, Crystal Structure, and Activity of Pyrazole-Based Inhibitors of p38 Kinase. *J. Med. Chem.* **2007**, *50* (23), 5712–5719. (b) McClure, K. F.; Letavic, M. A.; Kalgutkar, A. S.; Gabel, C. A.; Audoly, L.; Barberia, J. T.; Braganza, J. F.; Carter, D.; Carty, T. J.; Cortina, S. R.; Dombroski, M. A.; Donahue, K. M.; Elliott, N. C.; Gibbons, C. P.; Jordan, C. K.; Kuperman, A. V.; Labasi, J. M.; LaLiberte, R. E.; McCoy, J. M.; Naiman, B. M.; Nelson, K. L.; Nguyen, H. T.; Peese, K. M.; Sweeney, F. J.; Taylor, T. J.; Trebino, C. E.; Abramov, Y. A.; Laird, E. R.; Volberg, W. A.; Zhou, J.; Bach, J.; Lombardo, F. Structure–Activity Relationships of Triazolopyridine Oxazole p38 Inhibitors: Identification of Candidates for Clinical Development. *Bioorg. Med. Chem. Lett.* **2006**, *16* (16), 4339–4344. (c) McClure, K. F.; Abramov, Y. A.; Laird, E. R.; Barberia, J. T.; Cai, W.; Carty, T. J.; Cortina, S. R.; Danley, D. E.; Dipesa, A. J.; Donahue, K. M.; Dombroski, M. A.; Elliott, N. C.; Gabel, C. A.; Han, S.; Hynes, T. R.; LeMotte, P. K.; Mansour, M. N.; Marr, E. S.; Letavic, M. A.; Pandit, J.; Ripin, D. B.; Sweeney, F. J.; Tan, D.; Tao, Y. Theoretical and Experimental Design of Atypical Kinase Inhibitors: Application to p38 MAP Kinase. *J. Med. Chem.* **2005**, *48* (18), 5728–5737. (d) Dominguez, C.; Powers, D. A.; Tamayo, N. p38 MAP Kinase Inhibitors: Many Are Made, But Few Are Chosen. *Curr. Opin. Drug Discovery Dev.* **2005**, *8* (4), 421–430. (e) Dominguez, C.; Tamayo, N.; Zhang, D. p38 Inhibitors: beyond Pyridinylimidazoles. *Expert Opin. Ther. Pat.* **2005**, *15* (7), 801–816. (f) Goldstein, D. M.; Gabriel, T. Pathway to the Clinic: Inhibition of p38 MAP Kinase. A Review of Ten Chemotypes Selected for Development. *Curr. Top. Med. Chem.* **2005**, *5* (10), 1017–1029. (g) Hynes, J.; Leftheris, K. Small Molecule p38 Inhibitors: Novel Structural Features and Advances from 2002–2005. *Curr. Top. Med. Chem.* **2005**, *5* (10), 967–985. (h) Regan, J.; Breitfelder, S.; Cirillo, P.; Gilmore, T.; Graham, A. G.; Hickey, E.; Klaus, B.; Madwed, J.; Moriak, M.; Moss, N.; Pargellis, C.; Pav, S.; Proto, A.; Swinamer, A.; Tong, L.; Torcellini, C. Pyrazole Urea-Based Inhibitors of p38 MAP Kinase: From Lead Compound to Clinical Candidate. *J. Med. Chem.* **2002**, *45* (14), 2994–3008.
- (5) (a) Herberich, B.; Cao, G.-Q.; Chakrabarti, P.; Falsey, J.; Pettus, L.; Rzas, R. M.; Reed, A. B.; Reichelt, A.; Sham, K.; Thaman, M.; Wurz, R. P.; Xu, S.; Zhang, D.; Hsieh, F.; Lee, M. R.; Syed, R.; Li, V.; Grosfeld, D.; Plant, M. H.; Henkle, B.; Sherman, L.; Middleton, S.; Wong, L. M.; Tasker, A. S. Discovery of Highly Selective and Potent p38 Inhibitors Based on a Phthalazine Scaffold. *J. Med. Chem.* **2008**, *51*, 6271–6279. (b) Tasker, A.; Zhang, D.; Cao, G.; Chakrabarti, P.; Falsey, J. R.; Herberich, B. J.; Hungate, R. W.; Pettus, L. H.; Reed, A.; Rzas, R. M.; Sham, K. K. C.; Thaman, M. C.; Xu, S. Preparation of Phthalazine, Aza- and Diaza-phthalazine Compounds as Protein Kinase, Especially p38 Kinase, Inhibitors for Treating Inflammation and Related Conditions. PCT Int. Appl. WO 2006094187, 2006.
- (6) For other examples of Met-109 and Gly-110 “peptide flip”, see the following: (a) Fitzgerald, C. E.; Patel, S. B.; Becker, J. W.; Cameron, P. M.; Zaller, D.; Pikounis, V. B.; O'Keefe, S. J.; Scapin, G. Structural Basis for p38 α MAP Kinase Quinazolinone and Pyridol-Pyrimidine Inhibitor Specificity. *Nat. Struct. Biol.* **2003**, *10* (9), 764–769. (b) Bemis, G. W.; Salituro, F. G.; Duffy, J. P.; Harrington, E. M. Preparation of Pyrido[1,2-*c*]pyrimidin-3-ones or 1,2-Dihydro-pyrido[1,2-*c*]pyrimidin-3-ones as Inhibitors of p38. U.S. Patent 6147080, 2000. (c) A review on this subject can be found in the following: Lee, M. R.; Dominguez, C. MAP Kinase p38 Inhibitors: Clinical Results and an Intimate Look at Their Interactions with p38 α Protein. *Curr. Med. Chem.* **2005**, *12* (25), 2979–2994.
- (7) Alanine is rare as a floor residue in the ATP binding pocket. Only 7 out of the 518 kinases have alanine as the floor residue: Manning, G.; Whyte, D. B.; Martinez, R.; Hunter, T.; Sudarsanam, S. The Protein Kinase Complement of the Human Genome. *Science* **2002**, *298*, 1912–1916.
- (8) For references comparing DFG-in and DFG-out binding, see the following: (a) Tokarski, J. S.; Newitt, J. A.; Chang, C. Y. J.; Cheng, J. D.; Wittekind, M.; Kiefer, S. E.; Kish, K.; Lee, F. Y. F.; Borzilleri, R.; Lombardo, L. J.; Xie, D.; Zhang, Y.; Klei, H. E. The Structure of Dasatinib (BMS-354825) Bound to Activated ABL Kinase Domain Elucidates Its Inhibitory Activity against Imatinib-Resistant ABL Mutants. *Cancer Res.* **2006**, *66* (11), 5790–5797. (b) Nagar, B.; Bornmann, W. G.; Pellicena, P.; Schindler, T.; Veach, D. R.; Miller, W. T.; Clarkson, B.; Kuriyan, J. Crystal Structures of the Kinase Domain of c-Abl in Complex with the Small Molecule Inhibitors PD173955 and Imatinib (STI-571). *Cancer Res.* **2002**, *62* (15), 4236–4243.
- (9) Bakthavatchatam, R.; Blum, C. A.; Briellmann, H. L.; Caldwell, T. M.; De Lombaert, S. Preparation of Substituted Quinazolin-4-ylamine Analogs as VR1 Capsaicin Receptor Antagonists for Relieving Pain. PCT Int. Appl. WO 2003062209, 2003.
- (10) Ishiyama, T.; Ishida, K.; Miyaura, N. Synthesis of Pinacol Arylboronates via Cross-Coupling Reaction of Bis(pinacolato)diboron with Chloroarenes Catalyzed by Palladium(0)–Tricyclohexylphosphine Complexes. *Tetrahedron* **2001**, *57* (49), 9813–9816.
- (11) Fuerstner, A.; Leitner, A.; Mendez, M.; Krause, H. Iron-Catalyzed Cross-Coupling Reactions. *J. Am. Chem. Soc.* **2002**, *124* (46), 13856–13863.
- (12) Angell, R. M.; Baldwin, I. R.; Bamborough, P.; Deboeck, N. M.; Longstaff, T.; Swanson, S. Preparation of Fused Heteroaryls, in Particular Benzisoxazoles and Indazoles, for Use as p38 Kinase Inhibitors in the Treatment of Rheumatoid Arthritis. PCT Int. Appl. WO 2004010995, 2004.
- (13) Palermo, M. G. Novel One-Pot Cyclization of Ortho Substituted Benzonitriles to 3-Amino-1,2-benzisoxazoles. *Tetrahedron Lett.* **1996**, *37* (17), 2885–2886.
- (14) (a) Rahman, L. K. A.; Scrowston, R. M. 7-Substituted Benzo[*b*]thiophenes and 1,2-Benzisothiazoles. Part 1. Hydroxy- or Methoxy-Derivatives. *J. Chem. Soc., Perkin Trans. 1* **1983**, 2973–2977. (b) Rahman, L. K. A.; Scrowston, R. M. 7-Substituted Benzo[*b*]thiophenes and 1,2-Benzisothiazoles. Part 2. Chloro and Nitro Derivatives. *J. Chem. Soc., Perkin Trans. 1* **1984**, 385–390.
- (15) (a) Brown, H. S.; Galetin, A. J.; Hallifax, D.; Houston, J. B. Prediction of in Vivo Drug–Drug Interactions from in Vitro Data: Factors Affecting Prototypic Drug–Drug Interactions Involving CYP2C9, CYP2D6 and CYP3A4. *Clin. Pharmacokinet.* **2006**, *45* (10), 1035–1050. (b) Dresser, G. K.; Spence, J. D.; Bailey, D. G. Pharmacokinetic–pharmacodynamic consequences and clinical relevance of cytochrome P450 3A4 inhibition. *Clin. Pharmacokinet.* **2000**, *38* (1), 41–57.
- (16) (a) To generate the models, we used Amgen's internal FLAME software to generate the initial pose, then refined with molecular dynamics and scored with the MMGB energy function. For FLAME, see the following: Cho, S. J.; Sun, Y. FLAME: A Program To Flexibly Align Molecules. *J. Chem. Inf. Model.* **2006**, *46* (1), 298–306. (b) For the molecular dynamics optimization and MMGB scoring, see the following: Lee, M. R.; Sun, Y. Improving Docking Accuracy through Molecular Mechanics Generalized Born Optimization and Scoring. *J. Chem. Theory Comput.* **2007**, *3* (3), 1106–1119.
- (17) The incubation mixtures containing test article (1 μ M), rat or human liver microsomes (0.1 mg/mL), and potassium phosphate buffer (66.67 mM, pH 7.4) were prepared in bulk and dispensed into four different tubes to prepare triplicate samples and a blank (without NADPH) for each species. NADPH (1 mM) was added to start the incubations. Equal volume of acetonitrile containing 0.05% formic acid was added to each tube 10 min after the start of the incubation. The samples were then centrifuged, and the supernatants were transferred to the final sample plate for LCMS. The remainder of the test article was

- estimated by comparing the LCMS response of the test article in the incubation sample to the blank.
- (18) Kinase profiling on all kinases were tested at their apparent K_m of ATP, using 1 μM inhibitor. The kinase selectivity panel included p38(α , β , γ , δ), c-KIT, JNK(1,2,3), JAK(2,3), b-RAF, c-RAF, MAPKAPK2, KDR, SYK, RSK1, PI3K(α , δ), LCK, SRC, Aur(1,2), c-Met, TYK2, PIM2, ABL, FYN, LYN, ERK2, AKT1, BTK, PDGFR β . Of the 32 kinases tested, **3c** exhibited <50% percent of control against only four kinases (p38 α , p38 β , PDGFR β , and c-KIT). Further testing revealed that **3c** inhibited PDGFR β with an IC_{50} of 0.83 μM and c-KIT with an IC_{50} of 1.6 μM .
- (19) (a) Goldstein, D. M.; Alfredson, T.; Bertrand, J.; Browner, M. F.; Clifford, K.; Dalrymple, S. A.; Dunn, J.; Freire-Moar, J.; Harris, S.; Labadie, S. S.; La Fargue, J.; Lapierre, J. M.; Larrabee, S.; Li, F.; Papp, E.; McWeeney, D.; Ramesha, C.; Roberts, R.; Rotstein, D.; San Pablo, B.; Sjogren, E. B.; So, O.-Y.; Talamas, F. X.; Tao, W.; Trejo, A.; Villasenor, A.; Welch, M.; Welch, T.; Weller, P.; Whiteley, P. E.; Young, K.; Zipfel, S. Discovery of *S*-[5-Amino-1-(4-fluorophenyl)-1*H*-pyrazol-4-yl]-[3-(2,3-dihydroxypropoxy)phenyl]methanone (RO3201195), an Orally Bioavailable and Highly Selective Inhibitor of p38 Map Kinase. *J. Med. Chem.* **2006**, *49* (5), 1562–1575. (b) Liu, C.; Wroblewski, S. T.; Lin, J.; Ahmed, G.; Metzger, A.; Wityak, J.; Gillooly, K. M.; Shuster, D. J.; McIntyre, K. W.; Pitt, S.; Shen, D. R.; Zhang, R. F.; Zhang, H.; Doweyko, A. M.; Diller, D.; Henderson, I.; Barrish, J. C.; Dodd, J. H.; Schieven, G. L.; Leftheris, K. 5-Cyanopyrimidine Derivatives as a Novel Class of Potent, Selective, and Orally Active Inhibitors of p38 α MAP Kinase. *J. Med. Chem.* **2005**, *48* (20), 6261–6270.
- (20) Motulsky, H. J.; Christopoulos, A. Fitting Models to Biological Data Using Linear and Nonlinear Regression. *A Practical Guide to Curve Fitting*; Oxford University Press: New York, 2004.
- (21) (a) Perretti, M.; Duncan, G. S.; Flower, R. J.; Peers, S. H. Serum Corticosterone, Interleukin-1 and Tumor Necrosis Factor in Rat Experimental Endotoxemia: Comparison between Lewis and Wistar Strains. *Br. J. Pharmacol.* **1993**, *110* (2), 868–874. (b) Trentham, D. E.; Townes, A. S.; Kang, A. H. Autoimmunity to Type II Collagen an Experimental Model of Arthritis. *J. Exp. Med.* **1977**, *146* (3), 857–868.
- (22) Daylight Chemical Information Systems, Inc. <http://www.daylight.com>.
- (23) Cho, S. J.; Sun, X.; Harte, W. ADAAPT: Amgen's Data Access, Analysis, and Prediction Tools. *J. Comput.-Aided Mol. Des.* **2006**, *20*, 249–261.

JM8005405